Pair correlation of atoms scattered from colliding Bose-Einstein quasicondensates

Paweł Zin,[1,2] Tomasz Wasak,[3] Denis Boiron,[4] and Christoph I. Westbrook[4]
[1]*National Center for Nuclear Research, ul. Hoża 69, PL-00-681 Warsaw, Poland*
[2]*Faculty of Physics, University of Warsaw, ul. Pasteura 5, PL-02-093 Warsaw, Poland*
[3]*Max Planck Institute for the Physics of Complex Systems, Nöthnitzer Strasse 38, 01187 Dresden, Germany*
[4]*Université Paris-Saclay, Institut d'Optique Graduate School, Centre National de la Recherche Scientifique, Laboratoire Charles Fabry, 91127 Palaiseau Cedex, France*

(Received 1 August 2019; revised manuscript received 5 February 2020; accepted 2 March 2020; published 23 March 2020)

We consider elastic scattering of atoms from elongated clouds taking into account an effective, finite duration of the collision due to the expansion of the condensates. We also include the quasicondensate nature of the degenerate quantum gas, due to a finite temperature of the system. We evaluate the pair-correlation function measured experimentally in Kheruntsyan *et al.* [Phys. Rev. Lett. **108**, 260401 (2012)] and show that the finite duration of the collision is an important factor determining the properties of the correlations. Our analytic calculations are in agreement with the measurements. The analytical model we provide, useful for identifying physical processes that influence the correlations, is relevant for experiments with nonclassical pairs of atoms.

DOI: 10.1103/PhysRevA.101.033616

I. INTRODUCTION

Ultracold atoms offer a promising platform for studies of the foundations of quantum mechanics and also for applications that rely on quantum effects. The controlled generation of correlated pairs of atoms is an important method in this context, since such pairs play a similar role in quantum atomic physics as pairs of photons in quantum optics. The latter have been employed in tests of Bell's inequalities for photons [1], the photonic Hong-Ou-Mandel effect [2], and ghost imaging [3]. In the atomic context, generation of correlated pairs of atoms was reported [4–8], and it was shown theoretically and experimentally that they can be employed for demonstrating, for example, sub-Poissonian statistics of atoms [9,10], the violation of the atomic Cauchy-Schwarz inequality [11–14], the Hong-Ou-Mandel effect for atoms [15,16], and atomic ghost imaging [17,18]. The nonclassicality of the spatially separated, correlated atomic pairs has recently been employed for demonstration of Bell correlations [19], and for three-dimensional (3D) magnetic gradiometry [20]. Furthermore, the entangled pairs could find applications for the violation of Bell's inequality for massive particles [21,22], atomic interferometry [23], study of the quantum signatures of analog Hawking radiation [24], and other fundamental experimental tests of quantum mechanics such as the Einstein-Podolsky-Rosen gedanken experiment [25].

In our paper, we focus on a particular method of generating correlated pairs of atoms. In this scenario, the pairs are emitted from collisions of counterpropagating ultracold degenerate atomic Bose gases [7]. As a result of binary collisions between the particles that constitute the counterpropagating clouds, atomic pairs scatter out from the clouds with opposite velocities. In the spontaneous regime, where bosonic enhancement does not influence single collision events, the direction of velocity of outgoing particles is random. Due to the superposition principle, the quantum state of a single atomic pair is entangled in different momentum directions [25].

To further exploit the generated pairs of atoms, detailed control over the produced state of atomic pairs is required. To verify this control, some preliminary measurements are helpful. A particularly important example is provided by the observation of the correlation functions between pairs of atoms. Such properties of atoms scattered from colliding ultracold clouds were considered in the literature [10,26–39]. In particular, in the previous paper [32], we described an analytic calculation of pair-correlation functions. However, some of the results were in insufficient agreement with experimental results.

Since we published our work [32], we have refined and improved both the calculations and the experiment. From the experimental point of view, we have improved the signal to noise ratio, and simplified the collision geometry [11]. On the theory side, we are now able to take into account the expansion of the condensate during the collision, and show that the condensate expansion reduces the atom density and, therefore, also the collision rate. Thus, this effect limits the duration of collision and emission of pairs, and this finite time leads to an energy broadening of the decay products. We show that the broadening significantly improves the agreement between the theory and the experiment. Also, we take into account that when the system is highly elongated the phase of a degenerate Bose gas fluctuates on a scale shorter than the dimension of the cloud, resulting in a quasi-Bose-Einstein condensate. Finally, we include into the formalism the interaction of the scattered atoms with the mean-field potential of the colliding clouds, a factor that is often neglected. With our analytical treatment, we can identify the physical processes which affect the properties of the correlation functions.

The paper is organized as follows. In Sec. II, we introduce the experimental context (see Sec. II A) and the method used

to describe the quasicondensate (see Sec. II B), and calculate its most important properties. In Sec. III, we introduce the theoretical description of the quasicondensate collisions. Here, we postulate the variational ansatz that describes the evolution of the counterpropagating quasicondensates. In Sec. IV, we present the description of the scattered atoms based on the Bogoliubov method. There, we give analytical formulas for the pair-correlation function. It contains two types of correlations, which we shall label as "local" and "opposite" parts.[1] The local correlation involves atoms with nearly parallel momenta and is directly related to the single-particle correlation function. The opposite correlation involves the creation of pairs with nearly antiparallel momenta. In Sec. V, performing controlled approximations, and using a Gaussian variational ansatz, we derive formulas for the single-particle correlation function and local part of the pair-correlation function. In Sec. VI, proceeding in a similar way as in Sec. V, we derive formulas for the opposite part of the pair-correlation function. In Sec. VII, we apply the formulas obtained in the previous sections, and provide theoretical calculations of the normalized pair-correlation function that is measured in the experiment. We compare the theoretical and experimental results. We close the paper with a summary in Sec. VIII. Technical calculations are moved to the Appendices.

II. QUASICONDENSATE DESCRIPTION

A. Experimental setup

The details of the experimental setup are described in Ref. [11]. Briefly, a cigar-shaped BEC of metastable helium atoms in the $J = 1, m_J = 1$ state, containing $\approx 10^5$ atoms at temperature $T \approx 200\,\mathrm{nK}$, is initially trapped in a harmonic trap:

$$V(\mathbf{r}) = \tfrac{1}{2}m\left[\omega_r^2(x^2+y^2) + \omega_z^2 z^2\right], \tag{1}$$

where $\omega_r/2\pi = 1500\,\mathrm{Hz}$ and $\omega_z/2\pi = 7.5\,\mathrm{Hz}$. The trap is turned off and the atoms are transferred to the $m_J = 0$ state by a Raman transition (see Ref. [16]). The cloud is then split by Bragg diffraction into two packets with velocities differing by twice the single-photon recoil velocity $v_0 = 9.2$ cm/s along the axial (z) direction (see Fig. 1). Atoms interact via binary, s-wave collisions and scatter into a spherical halo the radius of which in velocity space is about the recoil velocity. The scattered atoms fall onto a detector that records the arrival times and positions of individual atoms with a quantum efficiency of $\approx 25\%$. We use the arrival times and positions to reconstruct 3D velocity vectors for each atom. The precision of the measurement is limited by a finite resolution of the detector. The resolution will be taken into account in our comparison between the theoretical estimates and the experimental results.

B. Bogoliubov method

Since the system is elongated along the z axis, we need to include the description of the phase fluctuations of the BEC. To this end, we divide the field operator into two parts $\hat{\Psi} = \hat{\Psi}_{\mathrm{QC}} + \hat{\delta}$ where $\hat{\Psi}_{\mathrm{QC}}$ describes the quasicondensate and $\hat{\delta}$ the scattered atoms. We describe the quasicondensate within Bogoliubov method in the density-phase representation [40], where

$$\hat{\Psi}_{\mathrm{QC}} = e^{i\hat{\phi}}\sqrt{\hat{n}} = e^{i\hat{\phi}}\sqrt{n+\delta\hat{n}} \tag{2}$$

where $n(\mathbf{r}) = \langle\hat{n}(\mathbf{r})\rangle$ is the mean density given by the solution of the Gross-Pitaevskii (GP) equation

$$-\frac{\hbar^2}{2m}\frac{\triangle\sqrt{n(\mathbf{r})}}{\sqrt{n(\mathbf{r})}} + V(\mathbf{r}) + g'n(\mathbf{r}) = \mu, \tag{3}$$

supplemented with the normalization condition $\int d\mathbf{r}\, n(\mathbf{r}) = N$. Here, the coupling strength $g' = \frac{4\pi\hbar^2 a'}{m}$, where a' denotes the s-wave scattering length, and the potential $V(\mathbf{r})$ is given by Eq. (1). In Eq. (2), $\hat{\delta}n$ and $\hat{\phi}$ are the density fluctuation and phase operators, respectively, which in the Bogoliubov approximation take the following forms:

$$\delta\hat{n}(\mathbf{r}) = \sqrt{n(\mathbf{r})}\sum_\nu [f_\nu^-(\mathbf{r})\hat{a}_\nu + \mathrm{H.c.}], \tag{4a}$$

$$\hat{\phi}(\mathbf{r}) = \frac{1}{\sqrt{4n(\mathbf{r})}}\sum_\nu [-if_\nu^+(\mathbf{r})\hat{a}_\nu + \mathrm{H.c.}], \tag{4b}$$

where "H.c." stands for the Hermitian conjugate. Here, $\hat{a}_\nu$ are the quasiparticle annihilation operators and $f_\nu^\pm$ are mode functions obtained via solution of the Bogoliubov–de Gennes equation. In the case of highly elongated condensates, it turns out that, to a very good approximation, the phase operator $\hat{\phi}(\mathbf{r})$ depends only on the longitudinal z coordinate [41]. In the regime where the thermal fluctuations dominate, the modes responsible for phase fluctuation are highly populated, and we can approximate the creation and annihilation operators

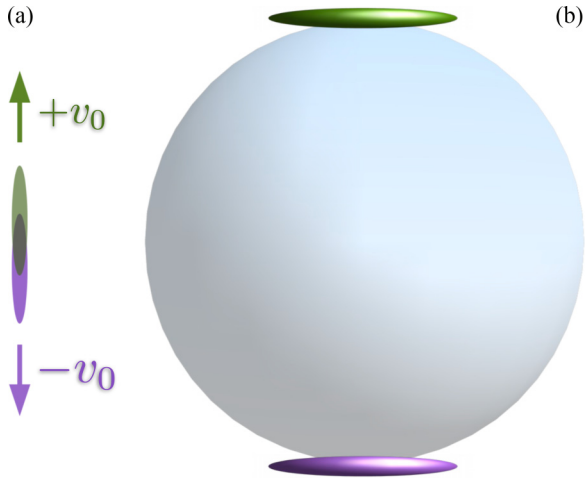

FIG. 1. Diagram of the collision geometry. (a) After Bragg diffraction, two cigar-shaped BECs move (in position space) at a relative velocity of $2v_0$ in the vertical (z) direction. Binary collisions scatter atoms isotropically from the BECs. (b) After expansion, the scattered atoms occupy a spherical halo (in momentum space), while the unscattered atoms from the BECs acquire a pancake shape and coincide with the extreme top and bottom of the halo. We compute correlations between scattered atoms on the halo, excluding the region near the BECs. The figures are not to scale.

[1] In the previous papers [9,11], we used the labels "collinear" and "back to back" instead of "local" and "opposite," respectively.

by c numbers [42], i.e., $\hat{a}_\nu \to \alpha_\nu$. This is done together with replacing the quantum average over the thermal state by an average over a thermal probability distribution, i.e.,

$$\langle \ldots \rangle \to \langle \ldots \rangle_{\rm cl} = \prod_\nu \int d^2\alpha_\nu \, P(\alpha_\nu) \ldots ,$$

where

$$P(\alpha_\nu) = \frac{\epsilon_\nu}{k_B T \pi} \exp\left(-\frac{\epsilon_\nu |\alpha_\nu|^2}{k_B T} \right). \tag{5}$$

As a result, we can replace the operator $\hat{\Psi}_{\rm QC}$ with a function $\psi_{\rm QC}$:

$$\hat{\Psi} = \psi_{\rm QC}(\mathbf{r}) + \hat{\delta}(\mathbf{r}), \tag{6}$$

where

$$\psi_{\rm QC}(\mathbf{r}) = \sqrt{n + \delta n(\mathbf{r})} e^{i\phi(\mathbf{r})}. \tag{7}$$

Here, the functions δn and ϕ are calculated from Eq. (4), with the operators replaced by c numbers drawn from the distribution given in Eq. (5).

We solve the GP equation (3) using the Gaussian variational ansatz of the form

$$n(\mathbf{r}) = \frac{N}{\pi^{3/2}\sigma_r^2\sigma_z} \exp\left(-\frac{x^2+y^2}{\sigma_r^2} - \frac{z^2}{\sigma_z^2} \right). \tag{8}$$

The solution, described in detail in Ref. [39], is

$$\sigma_r = a_{\rm hor}\left(1 + \sqrt{\frac{2}{\pi}} \frac{N a'}{\sigma_z} \right)^{1/4},$$

$$\left(\frac{\sigma_r \sigma_z}{a_{\rm hoz}^2} \right)^2 = \sqrt{\frac{2}{\pi}} \frac{N a'}{\sigma_z},$$

where $a_{\rm hor} = \sqrt{\hbar/m\omega_r}$ and $a_{\rm hoz} = \sqrt{\hbar/m\omega_z}$. Substituting the experimental values to the above equations, we obtain

$$\sigma_r \simeq 1.7\ \mu{\rm m}, \quad \sigma_z \simeq 0.3\ {\rm mm}, \quad \sigma_r/a_{\rm hor} \simeq 1.3.$$

Here, we have also used the experimentally determined value for the metastable helium s-wave scattering length, i.e., $a' = 7.51$ nm [43].

Due to the strong elongation of the cloud and the low temperature, only the longitudinal modes are excited. Therefore, we can approximately treat the system as quasi-one-dimensional, and define the one-dimensional density

$$n_{\rm 1D}(z) = \int dx dy \, n(\mathbf{r}) \tag{9}$$

and one-dimensional interaction constant

$$g_{\rm 1D} = g' \frac{\int d\mathbf{r}\, n^2(\mathbf{r})}{[\int d\mathbf{r} n(\mathbf{r})]^2}. \tag{10}$$

Substituting $n(\mathbf{r})$ given by Eq. (8) into Eqs. (9) and (10), we obtain $n_{\rm 1D} \simeq 2\times 10^8$ atoms/m and $g_{\rm 1D} n_{\rm 1D}/\hbar \simeq 2\pi \times 2500$ Hz, where $n_{\rm 1D}(z) = n_{\rm 1D} \exp(-z^2/\sigma_z^2)$. Using these values, we find $\gamma = m g_{\rm 1D}/\hbar^2 n_{\rm 1D}$, which is approximately equal to 2.5×10^{-5}, i.e., much smaller than unity. This places us in the weakly interacting regime, and justifies the use of the Bogoliubov method [40]. The thermal density fluctuations and coherence length of a uniform system take the form

$$\frac{\sqrt{\langle \delta n_{\rm 1D}^2 \rangle}}{n_{\rm 1D}} \simeq \gamma^{1/4} \sqrt{\frac{k_B T}{g_{\rm 1D} n_{\rm 1D}}}, \quad l_\phi = \frac{\hbar^2 n_{\rm 1D}}{m k_B T}. \tag{11}$$

We estimate the density fluctuations and coherence length of our system using the above formula, and obtain $\sqrt{\langle \delta n_{\rm 1D}^2 \rangle}/n_{\rm 1D} \simeq 0.09$ and $l_\phi \simeq 120\,\mu$m. Since the ratio $\sqrt{\langle \delta n_{\rm 1D}^2 \rangle}/n_{\rm 1D}$ is significantly smaller than unity, we neglect the density fluctuations in the further analysis. We emphasize that l_ϕ is smaller than the longitudinal size of the cloud but much larger than the transverse size of the cloud $2\sigma_r$. We additionally calculate the zero-temperature correlation length of the one-dimensional homogeneous system [44]:

$$l_\phi^{(0)} = \frac{\hbar}{\sqrt{m g_{\rm 1D} n_{\rm 1D}}} e^{2\pi/\sqrt{\gamma}}.$$

In our case $l_\phi^{(0)} \approx 10^{539}$ m (due to the exponent). The fact that $l_\phi^{(0)} \gg l_\phi$ justifies the use of classical field approximation as the thermal fluctuations dominate the quantum ones.

III. QUASICONDENSATE COLLISION

Anticipating that the number of scattered atoms is much smaller than the number of atoms from the quasicondensates (see Sec. VII), we neglect the impact of the scattered atoms on the colliding quasicondensates. In such a case the evolution of the classical field $\psi_{\rm QC}(\mathbf{r}, t)$ is given by the Gross-Pitaevskii equation:

$$i\hbar \partial_t \psi_{\rm QC}(\mathbf{r}, t) = \left(-\frac{\hbar^2}{2m}\triangle + g|\psi_{\rm QC}(\mathbf{r}, t)|^2 \right) \psi_{\rm QC}(\mathbf{r}, t). \tag{12}$$

Here, the interaction strength is given by $g = 4\pi\hbar^2 a/m$ and $a = 5.3$ nm is the scattering length between two atoms in the $m_J = 0$ state. The initial state is

$$\psi_{\rm QC}(\mathbf{r}, 0) \simeq \frac{1}{\sqrt{2}} \psi_{\rm QC}(\mathbf{r})(e^{iQz} + e^{-iQz}) \tag{13}$$

and describes a coherent splitting of a single cloud into two components; the function $\psi_{\rm QC}(\mathbf{r})$ is given by Eq. (7) and $Q = m v_0/\hbar$. It is convenient to factor out the rapidly oscillating phases in time and position, and rewrite the quasicondensate wave function in the following form:

$$\psi_{\rm QC}(\mathbf{r}, t) = \psi_{+Q}(\mathbf{r}, t) \exp\left(iQz - i\frac{\hbar Q^2}{2m} t \right) + \psi_{-Q}(\mathbf{r}, t) \exp\left(-iQz - i\frac{\hbar Q^2}{2m} t \right) \tag{14}$$

where $\psi_{\pm Q}$ are quasicondensate components moving with mean velocities $\pm v_0 \mathbf{e}_z$. In our situation, the momentum width of each of the components is much smaller than Q. Therefore, a measurement of the momentum density from $\psi_{\rm QC}$ would result in the observation of two separated components. In such a case, the slowly-varying-envelope approximation can be applied [45]. In Appendix A, we show that Eq. (12) can be

approximated and decomposed to take the form

$$i\partial_t \psi_{\pm Q} = \left(\mp\frac{\hbar^2}{m} Q\partial_z - \frac{\hbar^2}{2m}\triangle\right)\psi_{\pm Q} + g(|\psi_{\pm Q}|^2 + 2|\psi_{\mp Q}|^2)\psi_{\pm Q}. \quad (15)$$

As we shall see below, the time in which the density drops substantially is much smaller than the time needed for the wave packets to cross each other. Therefore, during the time important for the collision, the motion along the z direction is practically frozen. This allows us to neglect the terms containing derivatives $Q\partial_z$. As the normalization of each of the wave packets is the same and initially $\psi_{\pm Q}(\mathbf{r}, 0) = \frac{1}{\sqrt{2}}\psi_{\rm QC}(\mathbf{r})$ the above equations turn into a single one:

$$i\partial_t \psi(\mathbf{r}, t) = \left(-\frac{\hbar^2}{2m}\triangle + \frac{3}{2}g|\psi(\mathbf{r}, t)|^2\right)\psi(\mathbf{r}, t), \quad (16)$$

where the wave function

$$\frac{1}{\sqrt{2}}\psi = \psi_{+Q} = \psi_{-Q}, \quad (17)$$

with the normalization condition $\int d\mathbf{r}\,|\psi(\mathbf{r}, t)|^2 = N$ and initial condition $\psi(\mathbf{r}, 0) = \psi_{\rm QC}(\mathbf{r})$. We notice that Eq. (16) describes the ballistic expansion of the wave packet.

We have found above that the quasicondensate coherence length is much larger than the transverse size of the cloud. Therefore, we expect that the expansion of the cloud in the transverse directions is practically not affected by its quasicondensate nature. Thus, it is instructive to consider ballistic expansion of the condensate, i.e., the solution $\psi_c(\mathbf{r}, t)$ of the above Eq. (16) with the initial condition $\psi_c(\mathbf{r}, 0) = \sqrt{n(\mathbf{r})}$. We approach the problem with an approximate variational Gaussian ansatz, described in Ref. [39], and obtain

$$\psi_c(\mathbf{r}, t) \simeq \sqrt{\frac{N}{\pi^{3/2}\sigma_z(t)\sigma_r^2(t)}}\exp\left(-\frac{z^2}{2\sigma_z^2(t)} - ib_z(t)z^2\right) \times \exp\left[-\frac{x^2+y^2}{2\sigma_r^2(t)}\left(1 - i\tilde{\omega}t\frac{\sigma_r^2}{\tilde{a}_{\rm hor}^2}\right) - i\varphi(t)\right], \quad (18)$$

where

$$\sigma_r^2(t) = \sigma_r^2(1+\tilde{\omega}^2t^2), \quad \frac{\tilde{\omega}^2}{\omega_r^2} = \frac{1+\sqrt{\frac{2}{\pi}}\frac{3}{2}\frac{Na}{\sigma_z}}{1+\sqrt{\frac{2}{\pi}}\frac{Na'}{\sigma_z}},$$

$$\varphi(t) = \left(\frac{7}{4}\frac{\sigma_r^2}{\tilde{a}_{\rm hor}^2} - \frac{3}{4}\frac{\tilde{a}_{\rm hor}^2}{\sigma_r^2}\right)\arctan(\tilde{\omega}t),$$

and $\tilde{a}_{\rm hor} = \sqrt{\hbar/m\tilde{\omega}}$. With the parameters of the experiment, we obtain $\tilde{\omega} \simeq 1.02\omega_r$. This gives us the characteristic time of expansion $\tau_{\rm ex} = 1/\tilde{\omega} = 104\ \mu$s. This time allows us to estimate the change of the phase caused by thermal fluctuations. To this end, we consider a one-dimensional uniform system and calculate $\Delta\phi \equiv \sqrt{\langle[\phi(z=0,\tau_{\rm ex}) - \phi(z=0,0)]^2\rangle}$; the details of the evaluation are presented in Appendix B. There, we find that $\Delta\phi \simeq 0.14$, and since it is significantly smaller than unity we expect that the change of phase during the collision, caused by thermal fluctuations, is negligible. Thus, we assume that

$$\psi_{\rm QC}(\mathbf{r}, t) \simeq \psi_c(\mathbf{r}, t)e^{i\phi(z)}, \quad (19)$$

where $\psi_{\rm QC}(\mathbf{r}, t)$ and $\psi_c(\mathbf{r}, t)$ are the solutions of Eq. (16) with the two initial conditions: $\psi_{\rm QC}(\mathbf{r}, 0) = \psi_{\rm QC}(\mathbf{r}) = \sqrt{n(\mathbf{r})}e^{i\phi(z)}$ and $\psi_c(\mathbf{r}, 0) = \sqrt{n(\mathbf{r})}$.

Additionally, we find the expansion time $\tau_{\rm ex}$ to be much smaller than the time needed for the quasicondensates to cross each other, $2\sigma_z/v_0 \simeq 6$ ms. This justifies the use of the approximation which leads to Eq. (16).

We now make one more approximation. From the formulas presented in Ref. [39], we find that the phase gradient $b_z(\tau_c)\sigma_z$ is much smaller than $\partial_z\phi(z)$ and thus can be neglected. Additionally, we find that $\sigma_z(\tau_{\rm ex}) \simeq \sigma_z$. As a result, in what follows, we use $\psi_c(\mathbf{r}, t)$ given by Eq. (18) with $\sigma_z(t) \simeq \sigma_z$ and $b_z(t) \simeq 0$. For simplicity of the notation, we express the variational ansatz, given by Eq. (18), decoupling its z dependence:

$$\psi_c(\mathbf{r}, t) = \psi_\rho(\mathbf{r}_\perp, t)\exp\left(-\frac{z^2}{2\sigma_z^2}\right),$$

$$\psi_\rho(\mathbf{r}_\perp, t) = \sqrt{n_0}\frac{\sigma_r}{\sigma_r(t)}\exp\left[-i\varphi(t)\right] \times \exp\left[-\frac{x^2+y^2}{2\sigma_r^2(t)}\left(1 - i\tilde{\omega}t\frac{\sigma_r^2}{\tilde{a}_{\rm hor}^2}\right)\right], \quad (20)$$

where $\mathbf{r}_\perp = x\mathbf{e}_x + y\mathbf{e}_y$ and $n_0 = N/(\pi^{3/2}\sigma_z\sigma_r^2)$.

IV. THE SCATTERED ATOMS

We now turn our attention to the description of the scattering process. As in the experiment, we consider the scattered atoms with velocities restricted to $\frac{\pi}{3} < \theta < \frac{2\pi}{3}$, where θ is the angle between the velocity of the atoms and the z axis. Thus, the average distance traveled by the scattered atoms within the cloud is approximately given by $2\sigma_r \simeq 3.4\ \mu$m. This distance is much smaller than the mean free path equal to $1/(8\pi a^2 n_0) \simeq 66\ \mu$m. As a result, the system is in the collisionless regime and the use of the Bogoliubov approximation to treat the scattered atoms is adequate. The field operator $\hat{\delta}$, describing the scattered atoms, undergoes the time evolution given by

$$i\hbar\partial_t\hat{\delta}(\mathbf{r}, t) = H_0(\mathbf{r}, t)\hat{\delta}(\mathbf{r}, t) + B(\mathbf{r}, t)\hat{\delta}^\dagger(\mathbf{r}, t), \quad (21)$$

where

$$H_0(\mathbf{r}, t) = -\frac{\hbar^2}{2m}\triangle + 2g|\psi_{\rm QC}(\mathbf{r}, t)|^2, \quad (22)$$

$$B(\mathbf{r}, t) = g\psi_{\rm QC}^2(\mathbf{r}, t). \quad (23)$$

We assume that the initial state of the noncondensed particles is vacuum [46], i.e.,

$$\hat{\delta}(\mathbf{r}, 0)|0\rangle = 0. \quad (24)$$

Since the scattered atoms for chosen θ do not overlap with the quasicondensates, the pair-correlation function is given by the formula

$$G^{(2)}(\mathbf{r}_1, \mathbf{r}_2, t_f) = \langle\langle\hat{\delta}^\dagger(\mathbf{r}_1, t_f)\hat{\delta}^\dagger(\mathbf{r}_2, t_f)\hat{\delta}(\mathbf{r}_2, t_f)\hat{\delta}(\mathbf{r}_1, t_f)\rangle\rangle_{\rm cl}, \quad (25)$$

where we deal with quantum average over degrees of freedom described by the $\hat{\delta}$ operator and the classical average over quasicondensate modes. In the above, $t_f \simeq 0.3$ s is the time

it takes the atoms to reach the detector located 46 cm below the trapped cloud.

As the equation of motion for the field operator $\hat{\delta}$, given by Eq. (21), is linear, and the quantum state is the vacuum, the Wick theorem can be applied. As a result, the quantum average can be evaluated and it reads

$$\begin{aligned}&\langle\hat{\delta}^\dagger(\mathbf{r}_1,t_f)\hat{\delta}^\dagger(\mathbf{r}_2,t_f)\hat{\delta}(\mathbf{r}_2,t_f)\hat{\delta}(\mathbf{r}_1,t_f)\rangle\\&\quad=G^{(1)}(\mathbf{r}_1,\mathbf{r}_1,t_f)G^{(1)}(\mathbf{r}_2,\mathbf{r}_2,t_f)+|G^{(1)}(\mathbf{r}_1,\mathbf{r}_2,t_f)|^2\\&\qquad+|M(\mathbf{r}_1,\mathbf{r}_2,t_f)|^2,\end{aligned}\tag{26}$$

where

$$M(\mathbf{r}_1,\mathbf{r}_2,t_f)\equiv\langle\hat{\delta}(\mathbf{r}_1,t_f)\hat{\delta}(\mathbf{r}_2,t_f)\rangle\tag{27}$$

is called the anomalous density and

$$G^{(1)}(\mathbf{r}_1,\mathbf{r}_2,t_f)\equiv\langle\hat{\delta}^\dagger(\mathbf{r}_1,t_f)\hat{\delta}(\mathbf{r}_2,t_f)\rangle\tag{28}$$

is a single-particle correlation function of the scattered atoms in a single realization of the quasicondensate field.

In Eq. (26), two terms are responsible for the correlations: $|M(\mathbf{r}_1,\mathbf{r}_2,t_f)|^2$ and $|G^{(1)}(\mathbf{r}_1,\mathbf{r}_2,t_f)|^2$. The term $G^{(1)}(\mathbf{r}_1,\mathbf{r}_1,t_f)G^{(1)}(\mathbf{r}_2,\mathbf{r}_2,t_f)$ is a product of single-particle densities and represents uncorrelated particles. In the next sections, we show that the terms $|M(\mathbf{r}_1,\mathbf{r}_2,t_f)|^2$ and $|G^{(1)}(\mathbf{r}_1,\mathbf{r}_2,t_f)|^2$ represent the correlation of particles with opposite and collinear velocities, respectively. The appearance of correlations of particles with opposite velocities (which we shall call the "opposite" correlation) is due to the fact that particles are scattered in pairs of opposite momenta. On the other hand, the correlation of particles with collinear velocities (which we shall call the "local" correlation) is a bosonic bunching effect [36]. Therefore, we introduce notation $G^{(2)}_{\mathrm{op}}=|M|^2$ and $G^{(2)}_{\mathrm{loc}}=|G^{(1)}|^2$.

The scattering of atoms consists of two regimes. The first is the "spontaneous regime." Here, the atoms scatter into initially empty modes. The second is the "stimulated regime" where the atoms scatter into occupied modes. Here, the bosonic stimulation process comes into play and the scattering of atoms is greatly amplified. In the described experiment there are no signs of stimulated processes. Additionally, in Appendix F, we show the system is in the spontaneous regime. In such a case, the Heisenberg equation of motion, Eq. (21), can be solved within the first order of the perturbation theory [39]. Then, the formula for the anomalous density reads

$$\begin{aligned}M(\mathbf{r}_1,\mathbf{r}_2,t_f)=\frac{1}{i\hbar}\int_0^{t_f}dt\int d\mathbf{r}\,K(\mathbf{r}_1,t_f;\mathbf{r},t)\\\times K(\mathbf{r}_2,t_f;\mathbf{r},t)B(\mathbf{r},t),\end{aligned}\tag{29}$$

where $K(\mathbf{r}_1,t_1;\mathbf{r}_2,t_2)$ is the single-body propagator of the Hamiltonian from Eq. (22). Additionally, one obtains a simple relation between the one-body correlation function and the anomalous density:

$$G^{(1)}(\mathbf{r}_1,\mathbf{r}_2,t_f)=\int d\mathbf{r}\,M^*(\mathbf{r}_1,\mathbf{r},t_f)M(\mathbf{r},\mathbf{r}_2,t_f).\tag{30}$$

The above equation shows that the properties of the scattered atoms are described by the anomalous density M given by Eq. (29).

It turns out that it is easier to calculate the anomalous density in momentum space. The connection between both is given by the standard free propagator formula

$$\begin{aligned}M(\mathbf{R},\Delta\mathbf{R},t_f)=\frac{1}{(2\pi)^3}\int d\mathbf{K}\,d\Delta\mathbf{k}\,e^{i2\mathbf{K}\mathbf{R}}\\\times e^{i\frac{\Delta\mathbf{K}\Delta\mathbf{R}}{2}-i\frac{\hbar}{m}(K^2+\frac{\Delta K^2}{4})t_f}M(\mathbf{K},\Delta\mathbf{K}),\end{aligned}\tag{31}$$

where $\mathbf{R}=(\mathbf{r}_1-\mathbf{r}_2)/2$ and $\Delta\mathbf{R}=\mathbf{r}_1+\mathbf{r}_2$.

In Ref. [39], we analyzed the scattering of atoms from two colliding condensates (here we deal with quasicondensates). There, we employed a semiclassical approximation for the propagator K. The approximations used in construction of the propagator were the following. From Eq. (14), we find that the density $|\psi_{\mathrm{QC}}|^2$ present in the Hamiltonian H_0, which is given by Eq. (22), takes the form $|\psi_{\mathrm{QC}}|^2=|\psi_{+Q}|^2+|\psi_{-Q}|^2+\psi^*_{+Q}\psi_{-Q}e^{-2iQz}+\psi^*_{-Q}\psi_{+Q}e^{2iQz}$. The wave functions of the scattered atoms can be approximated by plane waves $e^{i\mathbf{k}\mathbf{r}}$ where $|\mathbf{k}|\simeq Q$. It seems intuitive that such a wave function "averages" the space on the length of $2\pi/Q$, thus averaging to zero the fringes $e^{\pm2iQz}$. In Ref. [39], we show, using the perturbation theory, that this indeed is true. As a result, we arrive at $|\psi_{\mathrm{QC}}|^2\simeq|\psi_{+Q}|^2+|\psi_{-Q}|^2$ and the Hamiltonian $H_0(\mathbf{r},t)\simeq-\frac{\hbar^2}{2m}\triangle+2g(|\psi_{+Q}|^2+|\psi_{-Q}|^2)$.

Now, we construct the propagator from the time-dependent solutions $\varphi_{\mathbf{k}}(\mathbf{r},t)$ of the single-particle Schrödinger equation $i\hbar\partial_t\varphi_{\mathbf{k}}=H_0\varphi_{\mathbf{k}}$. The next observation is the following. During the time needed for the scattered atom to leave the cloud, the change of the densities $|\psi_{\pm Q}|^2$ is negligible. This allows us to simplify the problem and construct the propagator from the solutions $\varphi_{\mathbf{k}}(\mathbf{r},t)$ of the time-independent Schrödinger equation $H_0\psi_{\mathbf{k}}(\mathbf{r},t)=\frac{\hbar^2k^2}{2m}\psi_{\mathbf{k}}(\mathbf{r},t)$. Here, we employ the semiclassical method and find an approximate solution of the Schrödinger equation presented in Appendix C. After constructing the propagator K from such solutions (which is a simple procedure), we insert it into Eq. (29) and arrive at (see Ref. [39])

$$\begin{aligned}M(\mathbf{K},\Delta\mathbf{K})=\frac{1}{i\hbar(2\pi)^3}\int_0^\infty dt\int d\mathbf{r}\\\times e^{-i\Delta\mathbf{K}\mathbf{r}+i\frac{\hbar}{m}(K^2+\frac{\Delta K^2}{4})t}\widetilde{B}(\mathbf{e}_{\mathbf{K}},\mathbf{r},t),\end{aligned}\tag{32}$$

where

$$\widetilde{B}(\mathbf{e}_{\mathbf{K}},\mathbf{r},t)=B(\mathbf{r},t)\exp\left[-i\Phi(\mathbf{r},\mathbf{e}_{\mathbf{K}},t)\right],\tag{33a}$$

$$\Phi(\mathbf{r},\mathbf{e}_{\mathbf{K}},t)=\frac{m}{\hbar^2Q}\int_{-\infty}^{\infty}ds\,V_{\mathrm{en}}(\mathbf{r}+s\mathbf{e}_{\mathbf{K}},t),\tag{33b}$$

$$V_{\mathrm{en}}(\mathbf{r},t)=2g[|\psi_{+Q}(\mathbf{r},t)|^2+|\psi_{-Q}(\mathbf{r},t)|^2],\tag{33c}$$

and $\mathbf{e}_{\mathbf{K}}=\frac{\mathbf{K}}{K}$. Here, $\psi_{\pm Q}$ are the two counterpropagating components of the quasicondensate. We notice the impact of the mean-field interaction $2g|\psi|^2$, which is present in the Hamiltonian H_0 in Eq. (22), is represented by the potential V_{en}, and enters the formulas through the phase Φ given by Eq. (33b). If we omitted the mean-field interaction in H_0, the phase Φ would be zero. Inserting Eqs. (17) and (19) into Eq. (33c), we finally arrive at

$$V_{\mathrm{en}}(\mathbf{r},t)=2g|\psi_c(\mathbf{r},t)|^2.\tag{34}$$

We now focus on the expression for $B(\mathbf{r},t)$. According to Eq. (23), we have $B(\mathbf{r},t)=g\psi^2_{\mathrm{QC}}(\mathbf{r},t)$. Inserting ψ_{QC}, given

by Eq. (14), we arrive at an expression with three terms. However, among them there is only one responsible for the scattering of atoms from collision between $\pm Q$ components. As we are interested only in this process, we neglect the rest, arriving at

$$B(\mathbf{r},t) \simeq 2g\psi_{+Q}\psi_{-Q}(\mathbf{r},t)\exp\left(-i\frac{\hbar Q^2}{m}t\right) = g\psi_c^2(\mathbf{r},t)\exp\left(2i\phi(z)-i\frac{\hbar Q^2}{m}t\right), \quad (35)$$

where we used Eqs. (17) and (19).

V. THE $G^{(1)}$ AND $G^{(2)}_{\rm loc}$ FUNCTIONS

We have

$$G^{(2)}_{\rm loc}(\mathbf{r}_1,\mathbf{r}_2,t_f) = \langle |G^{(1)}(\mathbf{r}_1,\mathbf{r}_2,t_f)|^2\rangle_{\rm cl}. \quad (36)$$

In order to calculate $G^{(1)}$, it is convenient to use the source function f description introduced in Ref. [39]. In classical physics, one can describe the single-particle properties of the source of particles by using a function $f(\mathbf{r},\mathbf{v},t)$ which describes the density of particles emitted by the source at time t and position $\mathbf{r}$ with velocity $\mathbf{v}$. For example, the rate of particle emission is given by $dN_{\rm sc}/dt = \int d\mathbf{r}\int d\mathbf{v}\, f(\mathbf{r},\mathbf{v},t)$. It can be easily shown using kinematics that the density of scattered particles in the $(\mathbf{r},\mathbf{v})$ space at time t_f denoted as $\varrho(\mathbf{r},\mathbf{v},t_f)$ is given by

$$\varrho(\mathbf{r},\mathbf{k},t_f) = \int_0^{t_f} dt\, f\left(\mathbf{r}-\frac{\hbar\mathbf{k}}{m}(t_f-t),\mathbf{k},t\right). \quad (37)$$

In Ref. [39], we found that it is convenient to define an analogous quantity in the quantum problem to describe the properties of scattered atoms. In order to do it, we need to have a semiclassical phase-space density of scattered atoms. The easiest choice of such density is the Wigner function. It is directly related to the single-particle correlation function through the formula

$$W(\mathbf{r},\mathbf{k},t_f) = \int \frac{d\mathbf{r}}{(2\pi)^3}\, e^{i\mathbf{k}\Delta\mathbf{r}}\, G^{(1)}\left(\mathbf{r}+\frac{\Delta\mathbf{r}}{2},\mathbf{r}-\frac{\Delta\mathbf{r}}{2},t_f\right). \quad (38)$$

Now, we define $f(\mathbf{r},\mathbf{k},t)$ as (one of the) functions satisfying

$$W(\mathbf{r},\mathbf{k},t_f) = \int_0^{t_f} dt\, f\left(\mathbf{r}-\frac{\hbar\mathbf{k}}{m}(t_f-t),\mathbf{k},t\right). \quad (39)$$

Now, from Eqs. (30)–(32), (38), and (39), we find that (for more details see Ref. [39])

$$f(\mathbf{r},\mathbf{k},t) = \frac{2}{(2\pi)^3\hbar^2}\int_{-t}^{t} d\Delta t\, e^{-i\frac{2\hbar k^2}{m}\Delta t} \times B_p^*(\mathbf{r},\mathbf{k},t,-\Delta t)B_p(\mathbf{r},\mathbf{k},t,\Delta t), \quad (40)$$

where

$$B_p(\mathbf{r},\mathbf{k},t,\Delta t) = \int d\Delta\mathbf{r}\, K_f(\Delta\mathbf{r},\Delta t) \times \widetilde{B}\left(\mathbf{e}_{\mathbf{k}},\mathbf{r}+\Delta\mathbf{r}+\frac{\hbar\mathbf{k}\Delta t}{m},t-\Delta t\right), \quad (41)$$

and K_f denotes the free propagator.

The next step is to obtain an analytic formula for f. This is done by introducing a number of approximations detailed in Appendix D. Here, we just summarize the main results. In Eq. (40), we notice the term $B_p^*B_p$, and a detailed analysis shows that the phase Φ cancels. Additionally, we find that the same happens with the phase $\phi(z)$. As a result, the function $G^{(1)}$, and consequently $G^{(2)}_{\rm loc}$ as well, does not depend on the realization of the thermal noise. This enables us to neglect the average $\langle\ldots\rangle_{\rm cl}$ while considering these averages. Thus, we have

$$G^{(2)}_{\rm loc}(\mathbf{r}_1,\mathbf{r}_2,t_f) = |G^{(1)}(\mathbf{r}_1,\mathbf{r}_2,t_f)|^2. \quad (42)$$

Finally, we use ψ_c given by Eq. (20) in order to obtain

$$f(\mathbf{r},\mathbf{k},t) = \frac{D_1}{(1+\tilde{\omega}^2t^2)^{3/2}\sin\theta}e^{-2\frac{z^2}{\sigma_z^2}-2\frac{x^2+y^2}{\sigma_r^2(t)}} \times \exp\left[-2\left(\frac{\delta k\sigma_r(t)}{\sin\theta}-\frac{x}{\sigma_r(t)}\tilde{\omega}t\frac{\sigma_r^2}{\tilde{a}_{\rm hor}^2}\right)^2\right], \quad (43)$$

where $D_1 = \frac{\sqrt{\pi}mg^2n_0^2\sigma_r}{4\sqrt{2}\pi^3\hbar^3Q}$, $\mathbf{e}_{\mathbf{k}} = (\sin\theta,0,\cos\theta)$, and $\delta k = k-Q$. One might wonder if the above function can be derived within a classical model, where one considers a collision of two clouds of atoms. It turns out that it is indeed the case, when one takes the Wigner function as the phase-space distribution of the colliding clouds [39].

Having the source function f, we now derive an approximate expression for the single-particle correlation function. We start with the inverted relation to that, which is given by Eq. (38) and reads

$$G^{(1)}\left(\mathbf{r}+\frac{\Delta\mathbf{r}}{2},\mathbf{r}-\frac{\Delta\mathbf{r}}{2},t_f\right) = \int d\mathbf{k}\, e^{-i\mathbf{k}\Delta\mathbf{r}}W(\mathbf{r},\mathbf{k};t_f).$$

We insert into that equation the function W from Eq. (39), and we obtain

$$\widetilde{G}^{(1)}(\mathbf{r},\Delta\mathbf{r},t_f) = \int_0^{t_f}dt\int d\mathbf{k}\, e^{-i\mathbf{k}\Delta\mathbf{r}}f\left(\mathbf{r}-\frac{\hbar\mathbf{k}}{m}(t_f-t),\mathbf{k},t\right),$$

where we denoted $G^{(1)}(\mathbf{r}+\frac{\Delta\mathbf{r}}{2},\mathbf{r}-\frac{\Delta\mathbf{r}}{2},t_f)$ by $\widetilde{G}^{(1)}(\mathbf{r},\Delta\mathbf{r},t_f)$. Moreover, introducing new variables $\mathbf{r}' = \mathbf{r}-\frac{\hbar}{m}\mathbf{k}(t_f-t)$, $\mathbf{k}_0 = \frac{m\mathbf{r}}{\hbar t_f}$, and $\Delta\mathbf{k}_0 = \frac{m\Delta\mathbf{r}}{\hbar t_f}$, we obtain

$$\widetilde{G}^{(1)}(\mathbf{r},\Delta\mathbf{r},t_f) = \int_0^{t_f}dt\int d\mathbf{r}'\left(\frac{m}{\hbar(t_f-t)}\right)^3 \times e^{-i\frac{1}{1-\frac{t}{t_f}}\left(\frac{\hbar}{m}\mathbf{k}_0t_f-\mathbf{r}'\right)\Delta\mathbf{k}_0}f\left(\mathbf{r}',\frac{\mathbf{k}_0-\frac{m\mathbf{r}'}{\hbar t_f}}{1-\frac{t}{t_f}},t\right). \quad (44)$$

Using Eq. (43) and the one above, we find that, if $\sigma_r \ll \sigma_z$, $\frac{m\sigma_z}{\hbar t_f} \ll \frac{1}{\sigma_r}$, and $\tilde{\omega}t_f \gg 1$, the above can be approximated as

$$\widetilde{G}^{(1)}\left(\frac{\hbar\mathbf{k}_0}{m}t_f,\frac{\hbar\Delta\mathbf{k}_0}{m}t_f,t_f\right) \simeq \left(\frac{m}{\hbar t_f}\right)^3\exp\left(-i\frac{\hbar}{m}\mathbf{k}_0\Delta\mathbf{k}_0t_f\right) \times \int_0^{t_f}dt\int d\mathbf{r}'\exp\left[i\Delta\mathbf{k}_0\left(\mathbf{r}'-\frac{\hbar}{m}\mathbf{k}_0t\right)\right]f(\mathbf{r}',\mathbf{k}_0,t). \quad (45)$$

With the experimental parameters, we verify that the conditions are satisfied, and this formula can be applied to our system.

Now, we proceed to the analysis of the density of scattered particles. From Eq. (45), we obtain

$$\varrho(\mathbf{k}) = \left\langle \widetilde{G}^{(1)}\left(\frac{\hbar\mathbf{k}}{m}t_f, 0, t_f\right)\right\rangle_{\rm cl} = \widetilde{G}^{(1)}\left(\frac{\hbar\mathbf{k}}{m}t_f, 0, t_f\right) \simeq \left(\frac{m}{\hbar t_f}\right)^3 \int_0^\infty dt \int d\mathbf{r}\, f(\mathbf{r}, \mathbf{k}, t).$$

Inserting f from Eq. (43) into the above, we obtain

$$\varrho(\mathbf{k}) = \left(\frac{m}{\hbar t_f}\right)^3 \frac{1}{\sin\theta} h\left(\frac{\delta k}{\sin\theta}\right), \tag{46}$$

where h is given by

$$h(\delta k) = D_2 \int_0^\infty \frac{d\tilde{t}}{\sqrt{\left(1+\tilde{t}^2\frac{\sigma_r^4}{\tilde{a}_{\rm hor}^4}\right)(1+\tilde{t}^2)}} \times \exp\left(-2\frac{\delta k^2\sigma_r^2(1+\tilde{t}^2)}{\left(1+\tilde{t}^2\frac{\sigma_r^4}{\tilde{a}_{\rm hor}^4}\right)}\right), \tag{47}$$

$D_2 = D_1(\frac{\pi}{2})^{3/2}\sigma_r^2\sigma_z/\tilde{\omega} = \frac{\pi}{Q}n_0^2a^2\sigma_r^3\tilde{a}_{\rm hor}^2\sigma_z$, and $\tilde{t} = \tilde{\omega}t$.

We additionally calculate the number of scattered atoms into the region where they are measured, i.e.,

$$N_{\rm sc} = \left(\frac{\hbar t_f}{m}\right)^3 \int_0^\infty k^2dk \int_{\pi/3}^{2\pi/3} \sin\theta d\theta \int_0^{2\pi} d\phi\, \rho(\mathbf{k}),$$

where $\mathbf{k} = k(\sin\theta\cos\phi, \sin\theta\sin\phi, \cos\theta)$. Upon inserting Eqs. (46) and (47) into the above and approximating $\int_0^\infty k^2dk = Q^2\int_{-\infty}^\infty d\delta k$, we arrive at

$$N_{\rm sc} = \frac{\pi^{7/2}}{\sqrt{2}} Q n_0^2 a^2 \sigma_r^2 \tilde{a}_{\rm hor}^2 \sigma_z. \tag{48}$$

Now, we focus on the normalized two-body correlation function measured in the experiment, and defined as

$$g^{(2)}_{\rm loc}(\Delta r_\perp, \Delta z) - 1 = \frac{\int d\tilde{\Delta}\mathbf{r}\, w(\Delta\mathbf{r} - \tilde{\Delta}\mathbf{r}) \int_V d\mathbf{r}\, G^{(2)}_{\rm loc}(\mathbf{r}_1, \mathbf{r}_2, t_f)}{\int d\tilde{\Delta}\mathbf{r}\, w(\Delta\mathbf{r} - \tilde{\Delta}\mathbf{r}) \int_V d\mathbf{r}\, G^{(1)}(\mathbf{r}_1, \mathbf{r}_1, t_f) G^{(1)}(\mathbf{r}_2, \mathbf{r}_2, t_f)}, \tag{49}$$

where $\mathbf{r}_1 = \mathbf{r} + \tilde{\Delta}\mathbf{r}/2$, $\mathbf{r}_2 = \mathbf{r} - \tilde{\Delta}\mathbf{r}/2$, and V denotes a volume where the spherical angles $\mathbf{r} = r(\sin\theta\cos\phi, \sin\theta\sin\phi, \cos\theta)$ are bounded by $\frac{\pi}{3} < \theta < \frac{2\pi}{3}$. The function $w(\mathbf{r})$ is given by

$$w(\mathbf{r}) = \frac{1}{(2\pi)^{3/2}\sigma_{zd}\sigma_{rd}^2} e^{-\frac{x^2+y^2}{2\sigma_{rd}^2} - \frac{z^2}{2\sigma_{zd}^2}} \tag{50}$$

and describes the detector resolution for two-particle detection. The transverse resolution is known to be $\sigma_{rd} = 350\ \mu$m [47]. The vertical resolution σ_{zd} has never been precisely measured, but from Ref. [4] we can place an upper limit $\sigma_{zd} < 60\ \mu$m. Due to the cylindrical symmetry of the system, $g^{(2)}_{\rm loc}$ depends only on $\Delta r_\perp = |\Delta\mathbf{r}_\perp|$ and Δz. Therefore, we denote it as $g^{(2)}_{\rm loc}(\Delta r_\perp, \Delta z)$.

VI. THE $G^{(2)}_{\rm op}$ FUNCTION

In this section, we consider

$$G^{(2)}_{\rm op}(\Delta\mathbf{R}, t_f) = \int d\mathbf{R}\, G^{(2)}_{\rm op}(\mathbf{R}, \Delta\mathbf{R}, t_f) = \int d\mathbf{R}\, \langle |M(\mathbf{R}, \Delta\mathbf{R}, t_f)|^2\rangle_{\rm cl}, \tag{51}$$

where

$$G^{(2)}_{\rm op}(\mathbf{R}, \Delta\mathbf{R}, t_f) = \langle |M(\mathbf{R}, \Delta\mathbf{R}, t_f)|^2\rangle_{\rm cl}, \tag{52}$$

with M given by Eq. (31).

However, at the first step, we consider the function $M(\mathbf{K}, \Delta\mathbf{K})$ given by Eq. (32). It can be decomposed into the following form:

$$M(\mathbf{K}, \Delta\mathbf{K}) \simeq M_\rho(\mathbf{K}, \Delta\mathbf{K}_\perp) M_z(\Delta K_z). \tag{53}$$

The detailed analysis of this function is performed in Appendix E1. The crucial step that leads to the above decomposition is that ψ_c given by Eq. (20) is of the Gaussian form and is decomposed into $(\mathbf{r}_\perp, t)$ and z parts. The second step is that the phase $\Phi(\mathbf{r}, \mathbf{e}_\mathbf{K}, t)$ can be effectively approximated by its average over z, i.e., $\Phi(\mathbf{r}, \mathbf{e}_\mathbf{K}, t) \to \widetilde{\Phi}(\mathbf{r}_\perp, \mathbf{e}_\mathbf{K}, t)$. Finally, we show that the term $\exp(-i\hbar\Delta K_z^2 t/4m)$, present in Eq. (32), may be neglected. From Eqs. (20), (33a), and (35), we notice (see Appendix E1 for more details) that these facts lead directly to a decomposition given by Eq. (53).

Inserting this decomposition into Eq. (31), we arrive at

$$M(\mathbf{R}, \Delta\mathbf{R}, t_f) = M_\rho(\mathbf{R}, \Delta\mathbf{R}_\perp, t_f) M_z(\Delta Z, t_f), \tag{54}$$

where

$$M_z(\Delta Z, t_f) = \int d\Delta K_z \exp\left(i\Delta K_z\frac{\Delta Z}{2} - i\frac{\hbar\Delta K_z^2}{4m}t_f\right) \times M_z(\Delta K_z), \tag{55}$$

$$M_\rho(\mathbf{R}, \Delta\mathbf{R}_\perp, t_f) = \frac{1}{(2\pi)^3}\int d\mathbf{K}\, d\Delta\mathbf{K}_\perp\, e^{i2\mathbf{K}\mathbf{R}} \times e^{i\frac{\Delta\mathbf{K}_\perp\Delta\mathbf{R}_\perp}{2} - i\frac{\hbar}{m}(K^2 + \frac{\Delta K_\perp^2}{4})t_f} M_\rho(\mathbf{K}, \Delta\mathbf{K}_\perp), \tag{56}$$

$$M_z(\Delta K_z) = \int dz \exp\left(-i\Delta K_z z + 2i\phi(z) - \frac{z^2}{\sigma_z^2}\right), \tag{57}$$

and $M_\rho(\mathbf{R}, \Delta\mathbf{R}_\perp, t_f)$ is given by Eq. (E6) from Appendix E1.

While calculating $G^{(2)}_{\rm op}(\mathbf{R}, \Delta\mathbf{R}, t_f)$, given by Eq. (52), we use the averaging $\langle\ldots\rangle_{\rm cl}$. From the definition of $M_z(\Delta K_z)$, we notice the presence of the phase $\phi(z)$, which depends on the realization. On the other hand, $\phi(z)$ is not present in M_ρ. Thus, the averaging $\langle |M(\mathbf{R}, \Delta\mathbf{R}, t_f)|^2\rangle_{\rm cl}$ influences only the M_z part. Because of that, we define

$$G_z^{(2)}(\Delta Z, t_f) = \langle |M_z(\Delta Z, t_f)|^2\rangle_{\rm cl}. \tag{58}$$

In Appendix E2, we show that

$$G_z^{(2)}(\Delta Z, t_f) = \int dK_z\, G_z^{(2)}\left(\Delta Z - \frac{\hbar t_f}{m}K_z, 0\right)\rho(K_z), \tag{59}$$

where $\rho(K_z) = \frac{2\pi l_\phi}{1+(K_z l_\phi/2)^2}$ is the velocity distribution directly related to the quasicondensate velocity distribution and

$G_z^{(2)}(\Delta Z, 0) = \exp(-\frac{\Delta Z^2}{2\sigma_z^2})$ is the initial correlation function. The above formula has a clear meaning. We start from the initial correlation function $G_z^{(2)}(\Delta Z, 0)$, which is proportional to the density of the quasicondensate in the z direction. At each point of the quasicondensate, we deal with the momentum distribution $\rho(K_z)$. Equation (59) describes how the correlation function changes due to the movement of particles with the initial distribution $\rho(K_z)$. The characteristic velocity of this distribution is $v_\phi = \hbar/ml_\phi$. Thus, for time t_f for which the distance $v_\phi t_f$ is much smaller than σ_z, the correlation function will not broaden much and should be given approximately by the initial distribution. In our case, $v_\phi t_f/\sigma_z \simeq 0.14$, which leads to a small broadening of the initial distribution, i.e., the Gaussian function fitted to the distribution

$$G_z^{(2)}(\Delta Z, t_f) \simeq (2\pi)^2 \frac{\sigma_z}{\tilde{\sigma}_z} \exp\left(-\frac{\Delta Z^2}{2\tilde{\sigma}_z^2}\right) \tag{60}$$

yields $\tilde{\sigma}_z \simeq 1.17\sigma_z$. Thus, we notice the practically negligible impact of the presence of the quasicondensate on $G_{\rm op}^{(2)}(\Delta\mathbf{R}, t_f)$.

For noninteracting particles and after sufficiently long expansion time, the cloud has the shape given by its velocity distribution. As a consequence, all the spatial correlations will be given by its momentum counterparts. Due to a large free-fall time, we might expect that this situation occurs also in our system, i.e., that $M(\mathbf{R}, \Delta\mathbf{R}, t_f)$ in position space is proportional to M in momentum space. If that happens, we say that the correlations are in the "far field." As we see above, in the case of ΔZ correlations the time t_f is too small. We are not in the far field for this variable (in fact we are almost in the "near field" as the correlations are given by the spatial density of the quasicondensate). In Appendix E3, we analyze the far-field conditions for other variables of the $M(\mathbf{R}, \Delta\mathbf{R}, t_f)$ function. We show that the approximate condition for ΔX, ΔY and $|\mathbf{R}|$ correlations to be in the far field is $\hbar\sigma_k^2 t_f/2m \gg 1$. Here σ_k is the correlation width in the momentum space. In Appendix E3, we find that $\sigma_{K_\perp} \approx \frac{\sqrt{2}}{\sigma_r}$ and $\sigma_K \approx \frac{2}{Q\tilde{a}_{\rm hor}^2}$. Substituting into the above experimental parameters, we find that for the above variables the conditions are satisfied. In such a case from Eqs. (31) and (54) we find

$$M_\rho(\mathbf{R}, \Delta\mathbf{R}_\perp, t_f) = CM_\rho(\mathbf{K}, \Delta\mathbf{K}_\perp) \tag{61}$$

where $\Delta\mathbf{R}_\perp = \frac{\hbar\Delta\mathbf{K}_\perp}{m} t_f$, $\mathbf{R} = \frac{\hbar\mathbf{K}}{m} t_f$, and $C = \frac{1}{2\sqrt{\pi}} (\frac{m}{i\hbar t_f})^{5/2} \exp[i(K^2 + \frac{\Delta\mathbf{K}_\perp^2}{4})\frac{\hbar t_f}{m}]$.

We define $G_\rho^{(2)}(\Delta\mathbf{R}_\perp, t_f)$ through the relation

$$G_{\rm op}^{(2)}(\Delta\mathbf{R}, t_f) = G_\rho^{(2)}(\Delta\mathbf{R}_\perp, t_f) G_z^{(2)}(\Delta Z, t_f). \tag{62}$$

Using Eqs. (51), (54), and (58), we arrive at

$$G_\rho^{(2)}(\Delta\mathbf{R}_\perp, t_f) = \int d\mathbf{R}\, |M_\rho(\mathbf{R}, \Delta\mathbf{R}_\perp, t_f)|^2. \tag{63}$$

We calculate this quantity in Appendix E4.

Finally, we note that the pair-correlation function measured in the experiment takes the form

$$g_{\rm op}^{(2)}(\Delta R_\perp, \Delta Z) = \frac{\int d\Delta\tilde{\mathbf{R}}\, w(\Delta\mathbf{R} - \Delta\tilde{\mathbf{R}}) G_{\rm op}^{(2)}(\Delta\mathbf{R}, t_f)}{\int d\Delta\tilde{\mathbf{R}}\, w(\Delta\mathbf{R} - \Delta\tilde{\mathbf{R}}) \int_V d\mathbf{R}\, G^{(1)}(\mathbf{r}_1, \mathbf{r}_1, t_f) G^{(1)}(\mathbf{r}_2, \mathbf{r}_2, t_f)} \tag{64}$$

where $\mathbf{r}_1 = \mathbf{R} + \Delta\tilde{\mathbf{R}}/2$, $\mathbf{r}_2 = -\mathbf{R} + \Delta\tilde{\mathbf{R}}/2$, and $\Delta R_\perp = |\Delta\mathbf{R}_\perp|$.

VII. RESULTS

To make a comparison between theory and experiment, we first examine $g_{\rm op}^{(2)}(0, 0)$, the amplitude of the opposite correlation, given by Eq. (64), and using Eqs. (62), (60), (E11), and (46).

In this case, the resolution, σ_{zd}, has a negligible effect on the width and will therefore be ignored. We obtain $g_{\rm op}^{(2)}(0) - 1 \simeq 0.087$. This is in poor agreement with the experimental value, $g_{\rm op}^{(2)}(0) - 1 = 0.16$. However, the value of $g_{\rm op}^{(2)}(0, 0) - 1$ depends crucially on the total number of particles in the quasicondensate, and the experimental value of the total number of particles has an uncertainty of about a factor of 2. Therefore, we seek the value of N which makes the theoretical and experimental $g_{\rm op}^{(2)}(0, 0)$ agree. We find $N \simeq 7\times10^4$, which is within the experimental uncertainty. From this value for N, we can deduce $\sigma_r/a_{\rm hor} \simeq 1.65\ \mu$m, $\sigma_z \simeq 0.26$ mm, $\tilde{\omega} \simeq 1.02\,\omega_r$, $l_\phi = 92\ \mu$m, $\tilde{\sigma}_z \simeq 1.23\,\sigma_z$, and $\Phi_0 \simeq 0.85$. We remind the reader that $a_{\rm hor} = \sqrt{\hbar/m\omega_r}$ is a harmonic oscillator length.

With the new value of N, we now calculate the other interesting characteristics. We start with the radial density profile, given by Eqs. (46) and (47). In Fig. 2, we plot the function $h(\delta k)$ normalized to unity. We find a half width of about $0.08\,Q$. The radial profile was not measured in Ref. [11], but a similar experiment, described in Ref. [37], has also found a value $0.08Q$ for this width. From Eq. (48) we find $N_{\rm sc} \simeq 2\times10^3$ atoms scattered in the region where the atoms are measured.

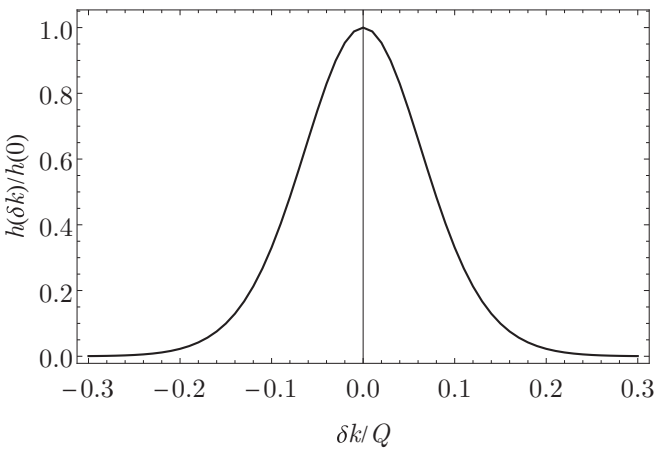

FIG. 2. The radial density profile $h(\delta k)/h(0)$ of the collision sphere as a function of the radial momentum in units of Q. The half width roughly equals $0.08\,Q$.

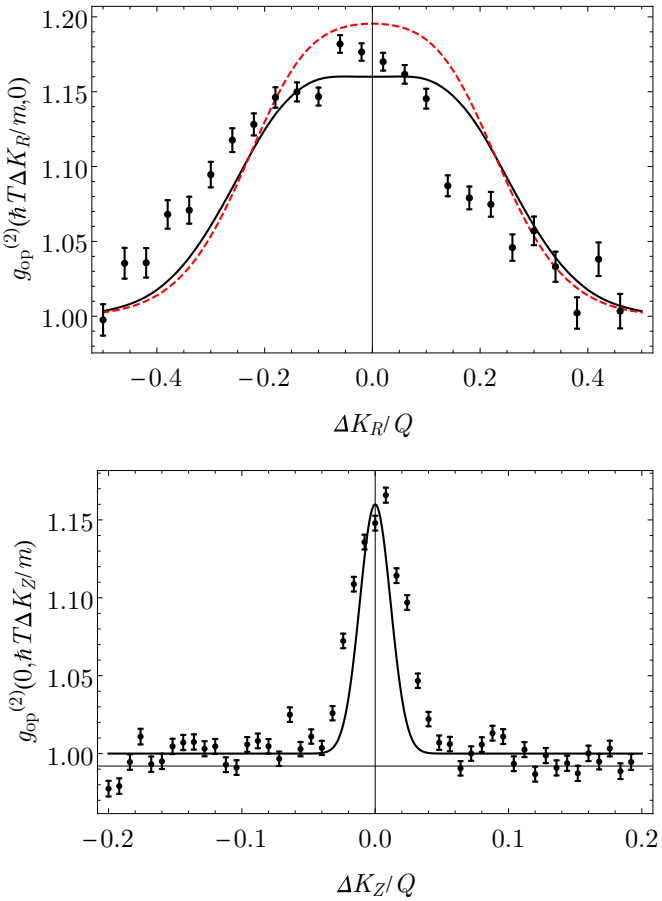

FIG. 3. The function $g_{\rm op}^{(2)}(\frac{\hbar t_f}{m}\Delta K_\perp, 0)$ (upper panel) and $g_{\rm op}^{(2)}(0, \frac{\hbar t_f}{m}\Delta K_Z)$ (lower panel) together with the experimental points as a function of $\Delta K_\perp/Q$ and $\Delta K_Z/Q$, respectively. The red dashed line shows $g_{\rm op}^{(2)}$ with the interaction term $2g|\psi_{\rm QC}(\mathbf{r},t)|^2$ present in Eq. (22) neglected.

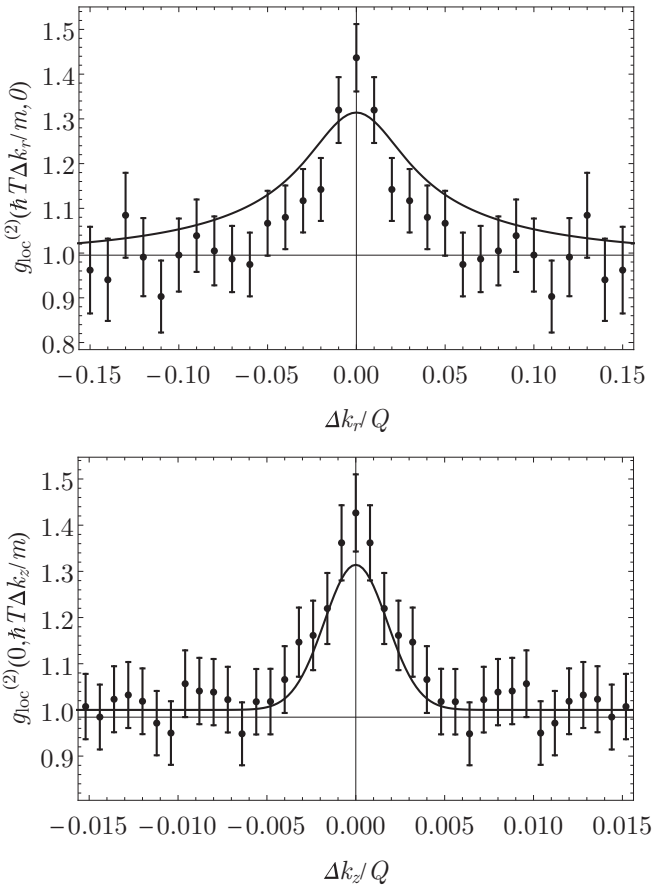

FIG. 4. The function $g_{\rm loc}^{(2)}(\frac{\hbar t_f}{m}\Delta k_\perp, 0)$ (upper panel) and $g_{\rm loc}^{(2)}(0, \frac{\hbar t_f}{m}\Delta k_z)$ (lower panel) together with the experimental points as a function of $\Delta k_\perp/Q$ and $\Delta k_z/Q$, respectively.

Next, we move to $g_{\rm op}^{(2)}(\Delta R_\perp, \Delta Z)$, the spatial dependence of the opposite correlation function. In Fig. 3, we plot $g_{\rm op}^{(2)}(\frac{\hbar t_f}{m}\Delta K_\perp, 0)$ and $g_{\rm op}^{(2)}(0, \frac{\hbar t_f}{m}\Delta K_Z)$ together with the experimental points. While leaving the collision volume, the atoms interact with the quasicondensate atoms via the mean-field potential $2g|\psi_{\rm QC}(\mathbf{r},t)|^2$ [present in the $H_0(\mathbf{r},t)$ given by Eq. (22)]. To see the influence of this interaction on the correlation function, we also plot $g_{\rm op}^{(2)}$ with $2g|\psi_{\rm QC}(\mathbf{r},t)|^2$ neglected (red dashed line in the upper panel of Fig. 3). The correlation in the radial direction (along $\Delta K_\perp$) measured in the experiment is quite close to our calculation, and we obtain slightly better agreement by including the mean field. The width in the radial direction is given by the width in velocity of the colliding condensates in that direction, that is, proportional to $1/\sigma_r$, the inverse of the radial condensate size.

In the case of the longitudinal (ΔK_Z) correlations, the theoretical width is smaller than the experimental one but not much. Unlike in the radial direction, the longitudinal width is approximately proportional to the size of the quasicondensate in that direction (equal approximately to σ_z). This is because for this correlation function the observation does not take place in the far field. To be in the far field, the time of flight must be longer than σ_z/v_ϕ where $v_\phi = \hbar/ml_\phi$ is the width of the quasicondensate velocity distribution. We find $vt_f/\sigma_z \simeq 0.14$ which locates these correlations much closer to the near field than to the far field. The remaining discrepancies may be due to the use of a variational approach. The ΔK_Z correlations are mostly given by the spatial size of the quasicondensate. The variational ansatz decreases the spatial width in the z direction compared to the true GP solution, and therefore overestimates the ΔK_Z width. Thus, using the GP solution the discussed difference would be smaller.

Finally, we examine the local correlation $g_{\rm loc}^{(2)}(\Delta r_\perp, \Delta z)$. From Eqs. (42), (43), (45)–(47), (49), and (50) we numerically calculate the $g_{\rm loc}^{(2)}$ function. In Fig. 4, we plot $g_{\rm loc}^{(2)}(\frac{\hbar t_f}{m}\Delta k_\perp, 0)$ and $g_{\rm loc}^{(2)}(0, \frac{\hbar t_f}{m}\Delta k_z)$ together with the experimental measurements. The local correlations are narrower than the opposite ones, and, therefore, the detector resolution is not negligible. The vertical resolution σ_{zd} is not well known, but we can find its value by fitting the data shown in Fig. 4 (lower panel). We find $\sigma_{zd} = 41\ \mu$m or approximately $0.0015v_0$ consistent with the limit set in Ref. [4].

The theoretical correlation function is in good agreement with the experimental result in the longitudinal direction while in the radial direction it is larger by a factor of 1.5. This is a marked improvement over the work given in Ref. [32], in which we estimated much smaller radial and longitudinal widths. This improvement is due to the inclusion of the

condensate expansion in the problem. As the condensate expands, the density declines to the point where the collision rate becomes negligible. Therefore, the effective duration of the collision is shorter, and this in turn increases the energy uncertainty of the collision products. The energy uncertainty broadens the correlation function relative to that calculated in Ref. [32], and it is still this uncertainty that determines the radial size of the correlation, rather than the spatial width of the source. In the case of the z direction, and under the experimental conditions, the correlation width is limited by the inverse of the size of the source, and in part also by the detector resolution. The calculated amplitude $g^{(2)}_{\rm loc}(0,0)$ is somewhat smaller than the measured one. As in the opposite correlation case, this may be due to the use of the variational ansatz. The fact that $g^{(2)}_{\rm loc}(0,0) < 2$ comes from the finite detector resolution. In the case of perfect detector resolution, i.e., $\sigma_{rd} = \sigma_{zd} = 0$, we have $g^{(2)}_{\rm loc}(0,0) = 2$.

VIII. SUMMARY

We have provided an analytical treatment of the production of atom pairs during the collision of two BECs via four-wave mixing and compared the results to an experiment. The calculation represents a significant improvement over our previous analytical calculation [32], and the agreement with the experiment is as good as an earlier numerical treatment [37]. Compared to the numerical approach, the present calculation has the advantage that we can identify the physical processes which affect the widths and amplitudes of the correlation functions. Compared to the earlier analytic treatment, we are now able to take into account the expansion of the condensate during the collision. The decrease in the density caused by the expansion is the mechanism which governs the collision time. Therefore, the uncertainty in the energy of the pairs is more accurately accounted for especially in the collinear correlation functions.

We are also able to clearly identify the role of the far-field condition. We have shown that the experiment is not in the far field for observation in the longitudinal (z) direction. Thus, the correlation along z for opposite pairs does not reflect the correlations in momentum, but rather more nearly the spatial correlations. For collinear pairs, the local correlation effect is simply a variant of the Hanbury-Brown-Twiss correlation [36], and the far-field condition plays no role. For example, Earth is not in the optical far field of typical stars in our galaxy. We thus find, as expected, that apart from broadening by the detector resolution, the local, longitudinal correlation width is a measure of the size of the source. The local correlation result also allows us to infer the detector resolution, which is in agreement with other upper limits we have already set.

We also took into account the interaction of the scattered atoms with the colliding clouds' mean-field potential. However, this did not affect the results much.

Finally, our treatment has included the fact that, in the experiments, the colliding clouds were quasicondensates, having a correlation length in the longitudinal direction smaller than the condensate itself. This feature, however, has not proved crucial for understanding the observations.

ACKNOWLEDGMENT

P.Z. acknowleges the support of the Mobility Plus program. D.B. and C.I.W. acknowledge funding by QuantERA Grant No. 18-QUAN-0012-01 (CEBBEC) and ANR Grant No. 15-CE30-0017 (HARALAB).

APPENDIX A: DERIVATION OF EQ. (15)

We insert Eq. (14) into Eq. (12), and arrive at

$$e^{iQz}\left[K - \frac{\hbar^2}{m}Q\partial_z + g(|\psi_{+Q}|^2 + 2|\psi_{-Q}|^2)\right]\psi_{+Q} + e^{-iQz}\left[K + \frac{\hbar^2}{m}Q\partial_z + g(|\psi_{-Q}|^2 + 2|\psi_{+Q}|^2)\right]\psi_{-Q} + ge^{-i3Qz}\psi^*_{+Q}\psi^2_{-Q} + ge^{i3Qz}\psi^*_{-Q}\psi^2_{+Q} = 0,$$

where $K = -i\hbar\partial_t - \frac{\hbar^2}{2m}\triangle$ and the factor $\exp(-i\frac{\hbar Q^2}{2m}t)$ multiplying the whole equation was dropped. In order to get the approximate equation for ψ_{+Q}, we multiply the equation by e^{-iQz}. We observe that ψ_{+Q} satisfies

$$i\hbar\partial_t\psi_{+Q} = \left(-\frac{\hbar^2}{m}Q\partial_z - \frac{\hbar^2}{2m}\triangle\right)\psi_{+Q} + g(|\psi_{+Q}|^2 + 2|\psi_{-Q}|^2)\psi_{+Q} + \cdots,$$

and the remaining terms at the right-hand side of the equation are always multiplied by some power of e^{iQz}. In the main part of the paper, we assumed that the momentum spread of $\psi_{\pm Q}$ is much smaller than Q. Thus, the remaining terms, due to rapid oscillations, effectively average to zero and can be neglected. As a result, we obtain Eq. (15).

APPENDIX B: TEMPORAL PHASE DIFFUSION OF THE QUASICONDENSATE

It follows directly from Ref. [40] that

$$\langle(\phi(z=0,t) - \phi(z=0,0))^2\rangle$$

caused by the thermal fluctuations reads

$$\langle(\phi(z=0,t) - \phi(z=0,0))^2\rangle = \frac{1}{n_{\rm 1D}\pi}\int dk\, n_k \frac{\varepsilon_k}{E_k}\sin^2\left(\frac{\varepsilon_k t}{\hbar}\right)$$

where $E_k = \hbar^2k^2/2m$, $\varepsilon_k = \sqrt{E_k(E_k + 2g_{\rm 1D}n_{\rm 1D})}$ and $n_k = [\exp(\varepsilon_k/k_BT) - 1]^{-1}$. Calculating the above for the parameters of the system considered in the paper and taking the expansion time $\tau_{\rm ex} = 1/\tilde{\omega}$ we obtain $\sqrt{\langle[\phi(z=0,\tau_{\rm ex}) - \phi(z=0,0)]^2\rangle} \simeq 0.14$.

APPENDIX C: DERIVATION OF THE ANOMALOUS DENSITY FORMULA

In this Appendix we show that the approximate treatment introduced in Ref. [39] in the case of collision of condensates applies also for our system. The crucial step of the analysis presented in Ref. [39] lies in the approximate solution to the single-particle scattering problem presented in Appendix C3

of Ref. [39]. There we deal with the equation

$$\left(-\frac{\hbar^2}{2m}\triangle + V_{\rm en}(\mathbf{r},t) - \frac{\hbar^2 k^2}{2m}\right)\varphi(\mathbf{r},t) = 0$$

with the boundary condition given by plane wave $e^{i\mathbf{kr}}$. In the above $V_{\rm en}$ is given by Eq. (34). Following Ref. [39] we introduce ϕ through the relation $\varphi = e^{i\mathbf{kr}+i\phi(\mathbf{r})}$. Substituting this form into the above equation and expanding ϕ in series $\phi = \phi^{(0)} + \phi^{(1)} + \cdots$ we obtain

$$2\mathbf{k}\nabla\phi^{(0)} = -\frac{2m}{\hbar^2}V_{\rm en},$$
$$2\mathbf{k}\nabla\phi^{(1)} = -(\nabla\phi^{(0)})^2 + i\triangle\phi^{(0)}$$

with formal solution

$$\phi^{(j)}(\mathbf{r},t) = -\frac{1}{2k}\int_{-\infty}^{0} ds\, W_j(\mathbf{r}+s\mathbf{e}_\mathbf{k},t) \tag{C1}$$

where $W_0 = \frac{2m}{\hbar^2}V_{\rm en}$ and $W_1 = (\nabla\phi^{(0)})^2 - i\triangle\phi^{(0)}$. We clearly see that $\phi^{(0)}$ depends on the $V_{\rm en}$ potential given by Eq. (34). We substitute to this equation ψ_c given by the variational ansatz and presented in Eq. (20). As a result in the case $\mathbf{e}_\mathbf{k} = \mathbf{e}_x$, $t = 0$, and $z = 0$ we obtain

$$\phi^{(0)}(x,y,0) = -\frac{2mgn_0\sigma_r}{\hbar^2 Q}\exp\left(-\frac{y^2}{\sigma_r^2}\right)\frac{\sqrt{\pi}}{2}\left[1+\mathrm{Erf}\left(\frac{x}{\sigma_r}\right)\right]$$

where $n_0 = N/(\pi^{3/2}\sigma_r^2\sigma_z)$. Inserting experimental values we obtain $\phi^{(0)}(\infty,0,0) \simeq 1.5$. We insert the above solution into Eq. (C1) and obtain the analytic form of $\phi^{(1)}(x,y,0)$. We find that $\phi^{(1)}(x,y,0)$ increases to infinity with the increase of x. This is a well-known phenomenon in semiclassical approximation caused by the presence of caustics. Anyway as stated in Ref. [39] we need the approximate solution only in the space where the cloud is present. This gives us roughly $x < 2\sigma_r$. In this part of space we find the maximal value of $\phi^{(1)}$ equal to 0.15. As this value is smaller than unity and also much smaller than $\phi^{(0)}$ we neglect it. Thus we have

$$\varphi_\mathbf{k} \simeq \exp[i\mathbf{kr} + i\phi^{(0)}(\mathbf{r})].$$

In Ref. [39] using the above formula we derived expression for the anomalous density given by Eqs. (32) and (31).

APPENDIX D: DERIVATION OF EQ. (43)

We now analyze the above formulas in a way analogous to that presented in Ref. [39]. It is crucial to note that $\widetilde{B}$ vanishes if $|x + \Delta x + \frac{\hbar k_x \Delta t}{m}|$ is larger than σ_r. As $\mathbf{k} = (k\sin\theta, 0, k\cos\theta)$ and $k \simeq Q$ with $\sin\theta > \sqrt{3}/2$, we find that $|\Delta t| < \Delta t_0 = \frac{2\sigma_r}{v_0\sqrt{3}} \simeq 20\ \mu$s. We note that Δt_0 is the time the scattered particle leaves the cloud. The characteristic distance $\Delta_0 = \sqrt{\hbar\Delta t_0/m} \simeq 0.56\ \mu$m present in the free propagator $K_f(x,t) \propto \exp\left(\frac{ix^2}{2\Delta_0^2 t/t_0}\right)$ is more than three times smaller than σ_r. On the distance Δ_0 and in time Δt_0, the change of the wave function ψ_c and the phase Φ is not crucial and can be neglected. As a result, from Eqs. (33a), (35), and (41), we obtain that

$$B_p(\mathbf{r},\mathbf{k},t,\Delta t) \simeq \widetilde{B}\left(\mathbf{e}_\mathbf{k}, \mathbf{r} + \frac{\hbar\mathbf{k}\Delta t}{m}, t\right)\exp\left(i\frac{\hbar Q^2}{m}\Delta t\right). \tag{D1}$$

In the formula describing the source function f, and given by Eq. (40), we notice the presence of the term $B_p^*(\mathbf{r},\mathbf{k},t,-\Delta t)B_p(\mathbf{r},\mathbf{k},t,\Delta t)$. According to the above equation, it is now equal to

$$\widetilde{B}^*\left(\mathbf{e}_\mathbf{k}, \mathbf{r} - \frac{\hbar\mathbf{k}\Delta t}{m}, t\right)\widetilde{B}\left(\mathbf{e}_\mathbf{k}, \mathbf{r} + \frac{\hbar\mathbf{k}\Delta t}{m}, t\right)\exp\left(i\frac{2\hbar Q^2}{m}\Delta t\right). \tag{D2}$$

Substituting here $\widetilde{B}$, given by Eqs. (33a) and (35), and using the fact that the phase Φ is constant along the $\mathbf{e}_\mathbf{k}$ direction, i.e., $\Phi(\mathbf{r} - s\mathbf{e}_\mathbf{k}, \mathbf{e}_\mathbf{k}, t) = \Phi(\mathbf{r}, \mathbf{e}_\mathbf{k}, t)$, we find a cancellation of the phase Φ in Eq. (D2). Additionally, $\frac{\hbar k_z \Delta t}{m}$ is maximally equal to σ_r. On that distance, we can neglect the change of the phase $\phi(z)$ and, as a result, we obtain a cancellation of the phase ϕ in Eq. (D2). As a result, we find that the quantity present in Eq. (D2) is equal to

$$g^2\psi_c^{2*}\left(\mathbf{r} - \frac{\hbar\mathbf{k}\Delta t}{m}, t\right)\psi_c^2\left(\mathbf{r} + \frac{\hbar\mathbf{k}\Delta t}{m}, t\right). \tag{D3}$$

Consequently, we find that the source function f does not depend on the phases Φ and ϕ. Due to the relation given by Eqs. (44) and (36), the same applies to a single-particle correlation function $G^{(1)}$ and the local part of pair-correlation function $G^{(2)}_{\rm loc}$. It means that these functions are not affected by the presence of the quasicondensate or the interaction of the scattered atoms with the atoms of the colliding clouds. Therefore, we can omit the bracket $\langle\ldots\rangle_{\rm cl}$ present in Eq. (36), and arrive at

$$G^{(2)}_{\rm loc}(\mathbf{r}_1,\mathbf{r}_2,t_f) = |G^{(1)}(\mathbf{r}_1,\mathbf{r}_2,t_f)|^2. \tag{D4}$$

We now continue with the analysis of the source function f. From Eqs. (40), (D1), and (D3), we find that

$$f(\mathbf{r},\mathbf{k},t) = \frac{2}{(2\pi)^3\hbar^2}\int_{-t}^{t} d\Delta t\, \exp\left(-i\frac{2\hbar(k^2-Q^2)}{m}\Delta t\right) \times g^2\psi_c^{*2}\left(\mathbf{r} - \frac{\hbar\mathbf{k}\Delta t}{m}, t\right)\psi_c{}^2\left(\mathbf{r} + \frac{\hbar\mathbf{k}\Delta t}{m}, t\right).$$

To proceed further, we make a series of approximations. First, $\frac{\hbar k_z \Delta t}{m}$ is maximally equal to σ_r. As $\sigma_r \ll \sigma_z$, we neglect the change of ψ_c on that distance. Second, Δt_0 is significantly smaller than the collision time. Therefore, we approximate $\int_{-t}^{t} \approx \int_{-\infty}^{\infty}$. Third, as $|k - Q| \ll Q$, we approximate $k^2 - Q^2 \simeq 2Q\delta k$, where $\delta k = k - Q$, and additionally approximate $\frac{\hbar\mathbf{k}\Delta t}{m} \simeq \frac{\hbar Q\Delta t}{m}\mathbf{e}_\mathbf{k}$. As a result, the above formula takes the form

$$f(\mathbf{r},\mathbf{k},t) = \frac{mg^2}{4\pi^3\hbar^3 Q}\int d\delta r\, \exp(-i4\delta k\delta r)\psi_c^{*2} \times (x - \delta r\sin\theta, y, z, t)\psi_c{}^2(x + \delta r\sin\theta, y, z, t),$$

where we introduced $\delta r = \frac{\hbar Q\Delta t}{m}$ and used $\mathbf{e}_\mathbf{k} = (\sin\theta, 0, \cos\theta)$. Inserting into the above ψ_c given by Eq. (20) and performing the integral over δr, we obtain

$$f(\mathbf{r},\mathbf{k},t) = \frac{D_1}{(1+\tilde{\omega}^2t^2)^{3/2}\sin\theta}e^{-2\frac{z^2}{\sigma_z^2} - 2\frac{x^2+y^2}{\sigma_r^2(t)}} \times \exp\left[-2\left(\frac{\delta k\sigma_r(t)}{\sin\theta} - \frac{x}{\sigma_r(t)}\tilde{\omega}t\frac{\sigma_r^2}{\tilde{a}_{\rm hor}^2}\right)^2\right], \tag{D5}$$

where $D_1 = \frac{\sqrt{\pi}mg^2n_0^2\sigma_r}{4\sqrt{2}\pi^3\hbar^3 Q} = \frac{2\sqrt{2}}{\sqrt{\pi}}n_0^2a^2\sigma_r\tilde{a}_{\rm hor}^2\frac{\tilde{\omega}}{Q}$.

APPENDIX E: THE CALCULATION OF THE $G^{(2)}_{\rm op}(\Delta\mathbf{R}, t_f)$ FUNCTION

1. Derivation of decomposition of $M(\mathbf{K}, \Delta\mathbf{K})$ functions

From Eqs. (32), (33a), and (35) we obtain

$$M(\mathbf{K}, \Delta\mathbf{K}) = \frac{g}{i\hbar(2\pi)^3}\int_0^\infty dt \int d\mathbf{r}\, \psi_c^2(\mathbf{r}, t)\exp(-i\Delta\mathbf{K}\mathbf{r}) \times \exp\left[i\frac{\hbar}{m}\left(K^2 - Q^2 + \frac{\Delta\mathbf{K}^2}{4}\right)t + 2i\phi(z) - i\Phi\right]. \tag{E1}$$

According to Eq. (20) $\psi_c(\mathbf{r}, t) = \psi_\rho(\mathbf{r}_\perp, t)\exp(-z^2/2\sigma_z^2)$. We insert this ψ_c into the above equation and concentrate on the integral over z which takes the form

$$\int dz\, \exp\left(-i\Delta K_z z - \frac{z^2}{\sigma_z^2} + 2i\phi(z) - i\Phi(\mathbf{r}, \mathbf{e}_\mathbf{K}, t)\right). \tag{E2}$$

First we start with phase Φ analysis. Due to the axial symmetry of the system we may take $\mathbf{e}_\mathbf{K} = (\sin\theta, 0, \cos\theta)$. As $\sigma_r \ll \sigma_z$ and $\sin\theta > \frac{\sqrt{3}}{2}$ we approximate

$$\Phi(\mathbf{r}, \mathbf{e}_\mathbf{K}, t) \simeq \frac{1}{\sin\theta}\Phi(\mathbf{r}, \mathbf{e}_x, t) = \frac{1}{\sin\theta}\frac{m}{\hbar^2 Q}\int_{-\infty}^\infty ds\, 2g|\psi_c(x+s, y, z, t)|^2$$

where we used Eqs. (33b) and (34). Inserting into the above the variational ansatz solution of ψ_c given by Eq. (20) we obtain

$$\Phi(\mathbf{r}, \mathbf{e}_\mathbf{K}, t) \simeq \frac{1}{\sin\theta}\frac{2gm}{\hbar^2 Q}\frac{n_0\sigma_r^2}{\sigma_r(t)}\sqrt{\pi}\exp\left(-\frac{y^2}{\sigma_r^2(t)} - \frac{z^2}{\sigma_z^2}\right). \tag{E3}$$

We find that the gradient of the phase $\phi(z)$ is much larger than $\partial_z\Phi$. This makes us approximate the integral given by Eq. (E2) as

$$\int dz\, \exp(-i\Delta K_z z)\exp\left(-\frac{z^2}{\sigma_z^2} + 2i\phi(z) - i\Phi(\mathbf{r}, \mathbf{e}_\mathbf{K}, t)\right) \approx \exp[-i\widetilde{\Phi}(\mathbf{r}_\perp, \mathbf{e}_\mathbf{K}, t)]M_z(\Delta K_z)$$

where

$$M_z(\Delta K_z) = \int dz\, \exp\left(-i\Delta K_z z - \frac{z^2}{\sigma_z^2} + 2i\phi(z)\right). \tag{E4}$$

In the above we used the variational ansatz wave function ψ_c given by Eq. (20). We also introduced $\widetilde{\Phi}(\mathbf{r}_\perp, \mathbf{e}_\mathbf{K}, t)$, which is $\Phi(\mathbf{r}, \mathbf{e}_\mathbf{K}, t)$ averaged over z with the condensate density $\exp(-\frac{z^2}{\sigma_z^2})$:

$$\widetilde{\Phi}(\mathbf{r}_\perp, \mathbf{e}_\mathbf{K}, t) = \frac{\int dz\, \Phi(\mathbf{r}, \mathbf{e}_\mathbf{K}, t)\exp\left(-\frac{z^2}{\sigma_z^2}\right)}{\int dz\, \exp\left(-\frac{z^2}{\sigma_z^2}\right)}.$$

Substituting Φ given by Eq. (E3) we obtain

$$\widetilde{\Phi}(\mathbf{r}_\perp, \mathbf{e}_\mathbf{K}, t) \simeq \Phi_0\frac{1}{\sin\theta\sqrt{1+\tilde{\omega}^2 t^2}}\exp\left(-\frac{y^2}{\sigma_r^2(t)}\right) \tag{E5}$$

where $\Phi_0 = \frac{2gmn_0\sigma_r}{\hbar^2 Q}\sqrt{\frac{\pi}{2}} \simeq 1.07$.

From Eq. (E4) we find that the characteristic width of ΔK_z is roughly equal to $1/l_\phi$. Using this value and taking as the time of the collision $1/\tilde{\omega}$ we estimate that the term $\frac{\hbar\Delta K_z^2}{4m}t$ present in Eq. (E1) is of the order of $\frac{\hbar}{4ml_\phi^2\tilde{\omega}} = \tilde{a}_{\rm hor}^2/4l_\phi^2 \ll 1$ and therefore can be neglected. With the above approximation $M(\mathbf{K}, \Delta\mathbf{K})$ given by Eq. (E1) turns into

$$M(\mathbf{K}, \Delta\mathbf{K}) = M_\rho(\mathbf{K}, \Delta\mathbf{K}_\perp)M_z(\Delta K_z)$$

where

$$M_\rho(\mathbf{K}, \Delta\mathbf{K}_\perp) = \frac{g}{i\hbar(2\pi)^3}\int_0^\infty dt \int d\mathbf{r}_\perp\, \exp(-i\Delta\mathbf{K}_\perp\mathbf{r}_\perp) \times \exp\left[i\frac{\hbar}{m}\left(K^2 - Q^2 + \frac{\Delta\mathbf{K}_\perp^2}{4}\right)t - i\widetilde{\Phi}(\mathbf{r}_\perp, \mathbf{e}_\mathbf{K}, t)\right]\psi_\rho^2(\mathbf{r}_\perp, t). \tag{E6}$$

2. The calculation of $\langle|M_z(\Delta Z, t_f)|^2\rangle_{\rm cl}$

Inserting Eq. (57) into Eq. (55) we find that

$$M_z(\Delta Z, t_f) = \int d\Delta K_z\, \exp\left(i\Delta K_z\frac{\Delta Z}{2} - i\frac{\hbar\Delta K_z^2}{4m}t_f\right) \times \int dz \exp\left(-i\Delta K_z z + 2i\phi(z) - \frac{z^2}{\sigma_z^2}\right).$$

Using the above we notice that $G_z^{(2)}(\Delta Z, t_f) = \langle|M_z(\Delta Z, t_f)|^2\rangle_{\rm cl}$ can be rewritten as

$$G_z^{(2)}(\Delta Z, t_f) = \int dK_z\, W\left(\Delta Z - \frac{\hbar t_f}{m}K_z, K_z\right) \tag{E7}$$

where

$$W(\Delta Z, K_z) = 2\pi\int d\Delta z\, \exp\left(-iK_z\Delta z - \frac{\Delta Z^2 + \Delta z^2}{2\sigma_z^2}\right) \times \left\langle \exp\left[2i\phi\left(\frac{\Delta Z + \Delta z}{2}\right) - 2i\phi\left(\frac{\Delta Z - \Delta z}{2}\right)\right]\right\rangle_{\rm cl}$$

is a Wigner function. Using local-density approximation we have

$$W(\Delta Z, K_z) \simeq \exp\left(-\frac{\Delta Z^2}{2\sigma_z^2}\right)\rho(K_z) \tag{E8}$$

where

$$\rho(K_z) = 2\pi\int d\Delta z\, \exp(-iK_z\Delta z) \times \left\langle \exp\left[2i\phi\left(\frac{\Delta z}{2}\right) - 2i\phi\left(-\frac{\Delta z}{2}\right)\right]\right\rangle_{\rm cl}.$$

The above can be calculated using the formulas for a 1D uniform system [48] arriving at

$$\rho(K_z) = \frac{2\pi l_\phi}{1 + (K_z l_\phi/2)^2}$$

where l_ϕ is the thermal coherence length given by Eq. (11).

For simplicity we rewrite Eq. (E7) as

$$G_z^{(2)}(\Delta Z, t_f) = \int dK_z\, G_z^{(2)}\left(\Delta Z - \frac{\hbar t_f}{m}K_z, 0\right)\rho(K_z)$$

where we used Eq. (E8) and $G_z^{(2)}(\Delta Z, 0) = \exp(-\frac{\Delta Z^2}{2\sigma_z^2})$.

3. Far-field conditions

In this Appendix we discuss far-field conditions for the $M_\rho(\mathbf{R}, \Delta\mathbf{R}_\perp, t_f)$ function given by Eqs. (56).

Following Ref. [39] we take the simple but realistic model of anomalous density

$$M_\rho(\mathbf{K}, \Delta\mathbf{K}_\perp, t_f) = M_0(t_f)\exp\left(-2\frac{(K-Q)^2}{\sigma_K^2}\right) \times \exp\left(-\frac{\Delta K_\perp^2}{2\sigma_{K_\perp}^2}\right) \quad \text{(E9)}$$

where $\sigma_{K_\perp} \approx \frac{\sqrt{2}}{\sigma_r}$ and $\sigma_K \approx \frac{2m}{\hbar Q\tau_d}$. Here τ_d is the characteristic time of the collision which in our case is equal to $1/\tilde{\omega}$. This gives $\sigma_K \approx \frac{2}{Q\tilde{a}_{\rm hor}^2}$. Inserting Eq. (E9) into Eq. (56) we arrive at

$$M(\mathbf{R}, \Delta\mathbf{R}, t_f) = M_0 M_1(\mathbf{R}, t_f) M_2(\Delta\mathbf{R}_\perp, t_f),$$

$$M_1(\mathbf{R}, t_f) = \int \frac{d\mathbf{K}}{(2\pi)^{3/2}} \exp\left(i2\mathbf{K}\mathbf{R} - i\frac{\hbar K^2}{m}t_f\right) \times \exp\left(-2\frac{(K-Q)^2}{\sigma_K^2}\right),$$

$$M_2(\Delta\mathbf{R}_\perp, t_f) = \frac{1}{(2\pi)^{3/2}}\int d\Delta\mathbf{K}_\perp \exp\left(i\frac{\Delta\mathbf{K}_\perp\Delta\mathbf{R}_\perp}{2}\right) \times \exp\left(-i\frac{\hbar\Delta K_\perp^2}{4m}t_f - \frac{\Delta K_\perp^2}{2\sigma_{K_\perp}^2}\right). \quad \text{(E10)}$$

As the above integrals are of Gaussian form they can be integrated analytically to get

$$M_1(\mathbf{R}, t_f) = \frac{Q\sigma_K}{4iR}\frac{1}{\sqrt{1+i\frac{\hbar\sigma_K^2 t_f}{2m}}}\exp\left(-i\frac{\hbar Q^2}{m}t_f\right) \times \exp\left(2iQR - \frac{(R-v_0t_f)^2\sigma_K^2}{2\left(1+i\frac{\hbar\sigma_K^2 t_f}{2m}\right)}\right)$$

and

$$M_2(\Delta\mathbf{R}_\perp, t_f) = \frac{1}{1+i\frac{\hbar\sigma_{K_\perp}^2 t_f}{2m}}\exp\left(-\frac{\Delta\mathbf{R}_\perp^2\sigma_{K_\perp}^2}{8\left(1+i\frac{\hbar\sigma_{K_\perp}^2 t_f}{2m}\right)}\right).$$

In the above we clearly notice that the far field is reached when $\frac{\hbar\sigma_K^2 t_f}{2m} \gg 1$ and $\frac{\hbar\sigma_{K_\perp}^2 t_f}{2m} \gg 1$. Substituting the experimental values we find

$$\frac{\hbar\sigma_K^2 t_f}{2m} \simeq 100, \qquad \frac{\hbar\sigma_{K_\perp}^2 t_f}{2m} \simeq 1.6\times10^3.$$

The above show that the far-field conditions are satisfied.

4. Calculation of $G_\rho^{(2)}(\Delta\mathbf{R}_\perp, t_f)$

Upon inserting Eq. (61) into (63) we arrive at

$$G_\rho^{(2)}(\Delta\mathbf{R}_\perp, t_f) = |C|^2\left(\frac{\hbar t_f}{m}\right)^3\int d\mathbf{K}\,|M_\rho(\mathbf{K}, \Delta\mathbf{K}_\perp, t_f)|^2$$

where we used $d\mathbf{R} = (\frac{\hbar t_f}{m})^3 d\mathbf{K}$. Now we insert M_ρ given by Eq. (E6) into the above and perform Dirac delta approximation described in Ref. [39] to obtain

$$G_\rho^{(2)}(\Delta\mathbf{R}_\perp, t_f) \simeq \left(\frac{m}{\hbar t_f}\right)^2\frac{mQ}{\hbar^3}\frac{1}{4(2\pi)^6}\int_0^\infty dt\int d\Omega_{\mathbf{K}} \times\left|\int d\mathbf{r}_\perp \exp[-i\Delta\mathbf{K}_\perp\mathbf{r}_\perp - i\widetilde{\Phi}(\mathbf{r}_\perp, \mathbf{e}_{\mathbf{K}}, t)]g\psi_\rho^2(\mathbf{r}_\perp, t)\right|^2.$$

Substituting ψ_ρ given by Eq. (20) into the above we find

$$G_\rho^{(2)}(\Delta\mathbf{R}_\perp, t_f) = C_0\int_0^\infty d\tilde{t}\int d\Omega_{\mathbf{K}}\frac{\pi}{(1+\tilde{t}^2)\sqrt{1+\tilde{t}^2\frac{\sigma_r^4}{\tilde{a}_{\rm hor}^4}}} \times\exp\left(-\frac{1}{2}\Delta K_\perp^2\cos^2\phi\frac{1+\tilde{t}^2}{1+\tilde{t}^2\frac{\sigma_r^4}{\tilde{a}_{\rm hor}^4}}\right) \times\left|\int d\tilde{y}\exp\left[-i\Delta K_\perp\sin\phi\tilde{y} - i\Phi(\theta, \sigma_r\tilde{y}, \tilde{t}/\tilde{\omega}) - \frac{\tilde{y}^2}{1+\tilde{t}^2}\left(1-i\tilde{t}\frac{\sigma_r^2}{\tilde{a}_{\rm hor}^2}\right)\right]\right|^2 \quad \text{(E11)}$$

where $\Delta R_\perp = |\Delta\mathbf{R}_\perp|$, $\Delta K_\perp = \frac{m\sigma_r\Delta R_\perp}{\hbar t_f}$, $\tilde{t} = \tilde{\omega}t$, $\tilde{y} = y/\sigma_r$, and

$$C_0 = \left(\frac{m}{\hbar t_f}\right)^2\frac{mQ}{\hbar^3}\frac{1}{4(2\pi)^6}(gn_0)^2\sigma_r^4.$$

In the above we used standard parametrization $\mathbf{e}_{\mathbf{K}} = (\sin\theta\cos\phi, \sin\theta\sin\phi, \cos\theta)$. It is important to mention that in the experiment the averaging over the solid angles $\Omega_{\mathbf{k}}$ is performed only over part of the sphere, i.e., for $\frac{\pi}{3} < \theta < \frac{2\pi}{3}$ [11].

We also calculate the above neglecting the phase Φ. Then it can be integrated arriving at

$$G_\rho^{(2)}(\Delta R_\perp, t_f) = \int_0^\infty d\tilde{t}\frac{2C_0\pi^3}{\left(1+\tilde{t}^2\frac{\sigma_r^4}{\tilde{a}_{\rm hor}^4}\right)}\exp\left(-\frac{1}{2}\Delta K_\perp^2\frac{1+\tilde{t}^2}{1+\tilde{t}^2\frac{\sigma_r^4}{\tilde{a}_{\rm hor}^4}}\right). \quad \text{(E12)}$$

APPENDIX F: SPONTANEOUS REGIME

In this Appendix, we show that the considered system is in the regime of spontaneous scattering of atoms. The system is in this regime when the mean number of scattered atoms per mode is much smaller than unity. In our case, the "mode" can be defined as the correlation volume of $G^{(1)}$ (see Ref. [39]). The maximal density of the scattered atoms in the momentum space is equal to $h(\delta k = 0)$. From Eq. (47), we find $h(0)/Q^3 \simeq 2200$ for the experimental parameters. Invoking the widths of $G_{\rm loc}^{(2)}$, we estimate the correlation volume as $(2\times0.05Q)^2(2\times0.003Q)$. Therefore, the mean number of atoms within the correlation volume (equal to 0.13) is much smaller than unity.

[1] A. Aspect, Nature (London) **398**, 189 (1999).

[2] C. K. Hong, Z. Y. Ou, and L. Mandel, Phys. Rev. Lett. **59**, 2044 (1987).

[3] B. I. Erkmen and J. H. Shapiro, Adv. Opt. Photon. **2**, 405 (2010).

[4] M. Bonneau, J. Ruaudel, R. Lopes, J.-C. Jaskula, A. Aspect, D. Boiron, and C. I. Westbrook, Phys. Rev. A **87**, 061603(R) (2013).

[5] R. Bücker, J. Grond, S. Manz, T. Berrada, T. Betz, C. Koller, U. Hohenester, T. Schumm, A. Perrin, and J. Schmiedmayer, Nat. Phys. **7**, 608 (2011).

[6] J. M. Vogels, K. Xu, and W. Ketterle, Phys. Rev. Lett. **89**, 020401 (2002).

[7] A. Perrin, H. Chang, V. Krachmalnicoff, M. Schellekens, D. Boiron, A. Aspect, and C. I. Westbrook, Phys. Rev. Lett. **99**, 150405 (2007).

[8] V. Krachmalnicoff, J.-C. Jaskula, M. Bonneau, V. Leung, G. B. Partridge, D. Boiron, C. I. Westbrook, P. Deuar, P. Ziń, M. Trippenbach, and K. V. Kheruntsyan, Phys. Rev. Lett. **104**, 150402 (2010).

[9] J.-C. Jaskula, M. Bonneau, G. B. Partridge, V. Krachmalnicoff, P. Deuar, K. V. Kheruntsyan, A. Aspect, D. Boiron, and C. I. Westbrook, Phys. Rev. Lett. **105**, 190402 (2010).

[10] P. Deuar, T. Wasak, P. Ziń, J. Chwedeńczuk, and M. Trippenbach, Phys. Rev. A **88**, 013617 (2013).

[11] K. V. Kheruntsyan, J.-C. Jaskula, P. Deuar, M. Bonneau, G. B. Partridge, J. Ruaudel, R. Lopes, D. Boiron, and C. I. Westbrook, Phys. Rev. Lett. **108**, 260401 (2012).

[12] T. Wasak, P. Szańkowski, P. Ziń, M. Trippenbach, and J. Chwedeńczuk, Phys. Rev. A **90**, 033616 (2014).

[13] T. Wasak, P. Szańkowski, M. Trippenbach, and J. Chwedeńczuk, Quantum Inf. Proc. **15**, 269 (2015).

[14] T. Wasak, A. Smerzi, and J. Chwedeńczuk, Sci. Rep. **8**, 1777 (2018).

[15] R. J. Lewis-Swan and K. V. Kheruntsyan, Nat. Commun. **5**, 3752 (2014).

[16] R. Lopes, A. Imanaliev, A. Aspect, M. Cheneau, D. Boiron, and C. I. Westbrook, Nature (London) **520**, 66 (2015).

[17] R. I. Khakimov, B. M. Henson, D. K. Shin, S. S. Hodgman, R. G. Dall, K. G. H. Baldwin, and A. G. Truscott, Nature (London) **540**, 100 (2016).

[18] S. S. Hodgman, W. Bu, S. B. Mann, R. I. Khakimov, and A. G. Truscott, Phys. Rev. Lett. **122**, 233601 (2019).

[19] D. K. Shin, B. M. Henson, S. S. Hodgman, T. Wasak, J. Chwedeńczuk, and A. G. Truscott, Nat. Commun. **10**, 4447 (2019).

[20] D. K. Shin, J. A. Ross, B. M. Henson, S. S. Hodgman, and A. G. Truscott, New J. Phys. **22**, 013002 (2020).

[21] R. J. Lewis-Swan and K. V. Kheruntsyan, Phys. Rev. A **91**, 052114 (2015).

[22] T. Wasak and J. Chwedeńczuk, Phys. Rev. Lett. **120**, 140406 (2018).

[23] T. Wasak, P. Szańkowski, R. Bücker, J. Chwedeńczuk, and M. Trippenbach, New J. Phys. **16**, 013041 (2014).

[24] D. Boiron, A. Fabbri, P.-É. Larré, N. Pavloff, C. I. Westbrook, and P. Ziń, Phys. Rev. Lett. **115**, 025301 (2015).

[25] M. Keller, M. Kotyrba, F. Leupold, M. Singh, M. Ebner, and A. Zeilinger, Phys. Rev. A **90**, 063607 (2014).

[26] V. A. Yurovsky, Phys. Rev. A **65**, 033605 (2002).

[27] R. Bach, M. Trippenbach, and K. Rzążewski, Phys. Rev. A **65**, 063605 (2002).

[28] P. Ziń, J. Chwedeńczuk, A. Veitia, K. Rzążewski, and M. Trippenbach, Phys. Rev. Lett. **94**, 200401 (2005).

[29] P. Ziń, J. Chwedeńczuk, and M. Trippenbach, Phys. Rev. A **73**, 033602 (2006).

[30] J. Chwedeńczuk, P. Ziń, K. Rzążewski, and M. Trippenbach, Phys. Rev. Lett. **97**, 170404 (2006).

[31] P. Deuar and P. D. Drummond, Phys. Rev. Lett. **98**, 120402 (2007).

[32] J. Chwedeńczuk, P. Ziń, M. Trippenbach, A. Perrin, V. Leung, D. Boiron, and C. I. Westbrook, Phys. Rev. A **78**, 053605 (2008).

[33] P. Deuar, J. Chwedeńczuk, M. Trippenbach, and P. Ziń, Phys. Rev. A **83**, 063625 (2011).

[34] A. A. Norrie, R. J. Ballagh, and C. W. Gardiner, Phys. Rev. Lett. **94**, 040401 (2005).

[35] A. A. Norrie, R. J. Ballagh, and C. W. Gardiner, Phys. Rev. A **73**, 043617 (2006).

[36] K. Mølmer, A. Perrin, V. Krachmalnicoff, V. Leung, D. Boiron, A. Aspect, and C. I. Westbrook, Phys. Rev. A **77**, 033601 (2008).

[37] A. Perrin, C. M. Savage, D. Boiron, V. Krachmalnicoff, C. I. Westbrook, and K. V. Kheruntsyan, New J. Phys. **10**, 045021 (2008).

[38] M. Ogren and K. V. Kheruntsyan, Phys. Rev. A **79**, 021606(R) (2009).

[39] P. Ziń and T. Wasak, Phys. Rev. A **97**, 043620 (2018).

[40] D. S. Petrov, D. M. Gangardt, and G. V. Shlyapnikov, J. Phys. IV (France) **116**, 5 (2004).

[41] F. Gerbier, Europhys. Lett. **66**, 771 (2004).

[42] T. Wasak, J. Chwedeńczuk, P. Ziń, and M. Trippenbach, Phys. Rev. A **86**, 043621 (2012).

[43] S. Moal, M. Portier, J. Kim, J. Dugue, U. D. Rapol, M. Leduc, and C. Cohen-Tannoudji, Phys. Rev. Lett. **96**, 023203 (2006).

[44] D. S. Petrov, G. V. Shlyapnikov, and J. T. M. Walraven, Phys. Rev. Lett. **85**, 3745 (2000).

[45] M. Trippenbach, Y. B. Band, and P. S. Julienne, Phys. Rev. A **62**, 023608 (2000).

[46] We neglect the quantum depletion of the condensates since we are interested in the scattered particles.

[47] M. Schellekens, R. Hoppeler, A. Perrin, J. Viana Gomes, D. Boiron, A. Aspect, and C. I. Westbrook, Science **310**, 648 (2005).

[48] I. Bouchoule, M. Arzamasovs, K. V. Kheruntsyan, and D. M. Gangardt, Phys. Rev. A **86**, 033626 (2012).